

GABAergic Interneurons of the Striatum

J.M. Tepper and T. Koós

Aidekman Research Center, Center for Molecular and Behavioral Neuroscience, Rutgers University,
Newark, NJ, United States

OUTLINE

| | | | |
|--|-----|---|-----|
| I. Introduction | 157 | <i>C. Afferents and Efferents</i> | 167 |
| II. Theoretical Issues: What Constitutes a Cell Type? | 158 | <i>D. Pharmacology</i> | 168 |
| III. PV-Immunoreactive Interneurons | 159 | VI. Striatal Tyrosine Hydroxylase Interneurons | 168 |
| <i>A. Neurocytology</i> | 159 | <i>A. Afferents and Efferents</i> | 170 |
| <i>B. Intrinsic Membrane Properties</i> | 159 | <i>B. Synaptic Connectivity</i> | 170 |
| <i>C. Firing Characteristics</i> | 159 | <i>C. Pharmacology</i> | 170 |
| <i>D. Afferents and Efferents</i> | 161 | VII. Fast Adapting Interneurons | 171 |
| <i>E. Synaptic Connectivity</i> | 161 | <i>A. Neurocytology</i> | 171 |
| <i>F. In Vivo Recordings</i> | 163 | <i>B. Afferents, Efferents, and Synaptic Connectivity</i> | 171 |
| <i>G. Pharmacology</i> | 164 | <i>C. Pharmacology</i> | 171 |
| IV. NPY Interneurons | 164 | VIII. Calretinin Interneurons | 171 |
| <i>A. Neurocytology</i> | 164 | IX. Recurrent Interneurons | 173 |
| <i>B. Intrinsic Membrane Properties</i> | 166 | X. Functional Considerations | 173 |
| <i>C. Afferents and Efferents</i> | 166 | XI. Summary and Conclusions | 174 |
| <i>D. Synaptic Connectivity</i> | 166 | Acknowledgments | 175 |
| <i>E. Pharmacology</i> | 167 | References | 175 |
| V. NPY-Neurogliaform Interneurons | 167 | | |
| <i>A. Neurocytology</i> | 167 | | |
| <i>B. Intrinsic Membrane Properties</i> | 167 | | |

I. INTRODUCTION

One of the areas in which our understanding of the structure and function of the striatum is undergoing the most rapid expansion and change is in the identification and characterization of striatal interneurons, their synaptic connectivity, and the role(s) that they play in the organization and control of striatal output.

First shown by strong uptake of radiolabeled GABA (Bolam et al., 1983) and subsequently by immunoreactivity for GABA and/or the GABA synthetic enzyme glutamic acid decarboxylase (GAD) (Bolam et al., 1985; Cowan et al., 1990; Kita, 1993), a population of striatal GABAergic interneurons comprising only a small fraction of all the striatal neurons was identified, and subsequently recognized as parvalbumin (PV)-expressing

fast-spiking interneurons (FSIs) (see chapter: Cell Types in the Different Nuclei of the Basal Ganglia). FSIs and the other striatal GABAergic interneurons have become the focus of a large number of anatomical and electrophysiological studies. Results from these experiments, most of them performed over the past 15 years, led to the view that although few in number, striatal GABAergic interneurons play a crucial role in regulating excitability and spike timing in the spiny projection neurons (traditionally referred to as medium spiny neurons, MSNs; see chapter: The Striatal Skeleton: Medium Spiny Projection Neurons and Their Lateral Connections) through feedforward inhibition (for reviews, see [Tepper et al., 2004, 2008](#)). More recently, several new classes of GABAergic interneurons have been identified and characterized. This review will focus on the anatomy, physiology, and synaptic connections and interactions of striatal GABAergic interneurons and suggests that striatal GABAergic interneurons should be viewed as having functions in addition to that of simple feedforward inhibition of MSN output.

II. THEORETICAL ISSUES: WHAT CONSTITUTES A CELL TYPE?

Initial attempts aimed at classifying GABAergic interneurons in the brain relied on a number of well-motivated but incorrect assumptions. Most importantly, it was expected that the expression of neurochemical markers, electrophysiological properties, and morphology would be systematically correlated among cell types. Instead, however, it is clear today that strict correlation among these characteristics is the exception not the rule, and individual “cell types” need to be defined using multiple dimensions. For instance, cell types that have gross differences in morphology and functional connectivity (for instance, neocortical basket cells and Martinotti cells) can exhibit the same electrophysiological properties, and conversely, single morphological types can be subdivided according to their electrophysiological and/or neurochemical characteristics. Recognition of this complexity motivated the currently predominant multidimensional approach to classification. To identify appropriate metrics for classification and to develop a commonly shared nomenclature among investigators, a complex scheme was introduced for cortical interneurons by the [Petilla Interneuron Nomenclature Group \(2008\)](#).

While the remarkable progress made in understanding GABAergic systems of the hippocampus and neocortex attest to the usefulness of this approach, the expectation that a complete classification will ultimately be achievable with this approach is called into question

by the observation that in many cases individual neurons are difficult or impossible to classify. One reasonable answer to this challenge, of course, is to attribute atypical characteristics simply to artifacts and “noise” introduced by the methods employed, or to the incompleteness of available information. Underlying this explanation is a conception of interneuron types that is analogous to Platonic forms, canonical configurations of characteristics of which individual interneurons are reasonable but imperfect approximations. In other words what a particular cell does can be fully captured by recognizing what type it belongs to with the idiosyncratic characteristics of the neuron introducing only quantitative not qualitative modifications. If this concept applies to all interneurons it can be expected that technological improvements will ultimately allow disambiguation of the identity of all interneurons.

Alternatives to this model are possible, however, and have significant implications for the more challenging cases of classification. In particular, it can be argued that the concept of a “neuronal type” would be better conceived in terms of the distinct developmental program or algorithm that controls the differentiation of the neuron. Although under some conditions this model would predict the existence of the phenotypically recognizable cell types consistent with the traditional approach; this model also accommodates the possibility that some interneurons may not exhibit multimodal or discontinuous distributions within phenotypic space characteristics. Semi-continuous distribution of properties may arise, for instance, if after a certain stage of differentiation, individual neurons adjust their intrinsic properties to achieve genetically defined set points in the global functioning of the network through appropriate responses to environmental signals that communicate the evolving network state, as they are almost certain to do (see [Marder and Goaillard, 2006](#)). As a result, various properties may develop that reflect idiosyncratic adaptations that the neuron happened to make to the varying spatial and temporal context of its resident local network during development. As a consequence, these neurons may not conform to any phenotypically recognizable types or classes and exhibit high degrees of variability and apparently random combinations of distinctive properties. Yet, these neurons would be executing the same function defined in terms of their homeostatic role.

Possible examples might include quantitative or qualitative variation in the expression of different ion channel subunits and resulting firing characteristics, depending on the magnitude or temporal pattern of excitatory drive to a local network or the extent and patterning of axon arborization determined by local variation in the density of similarly programmed interneurons. The phenotypic variability may be

particularly prominent if simultaneous adaptive processes operate in multiple interneurons with partially overlapping effects on network dynamics and function. The main implication for the issue of classification is that without understanding the developmental algorithms and in the absence of means for identifying them in individual neurons, classification may not be possible.

Since the classification of striatal interneurons is in many respects in its infancy, we feel that following the traditional Platonic approach is currently well justified and was applied in this chapter. Nevertheless, we caution against the expectation that a sufficiently detailed phenotypical characterization may ultimately render all interneurons classifiable and suggest that some of the already emerging problems, such as the classification of HT3aR-Cre targeted interneurons, may not be solved until appropriate developmental and/or genetic analysis becomes feasible.

III. PV-IMMUNOREACTIVE INTERNEURONS

A. Neurocytology

PV-immunoreactive (PV+) striatal interneurons (Fig. 8.1) are medium to large sized, averaging 16–18 μm in diameter. These were the striatal GABAergic neurons originally identified by their high affinity uptake of GABA (Bolam et al., 1983) and subsequently by the strongest immunoreactivity for GAD67 and GABA of any striatal neuron (Bolam et al., 1985; Cowan et al., 1990; Kita, 1993; Kubota et al., 1993). PV+ neurons do not express any of the other markers that identify the other types of striatal GABA interneurons, that is, calretinin (CR), nitric oxide synthase (NOS), somatostatin (SOM), or neuropeptide Y (NPY). Striatal PV+ interneurons issue 5–8 aspiny, often varicose dendrites that taper rapidly and branch relatively sparsely, that form a restricted dendritic arborization only 200–300 μm in diameter. The axon issues from the soma or proximal dendrite and branches repeatedly forming an extremely dense, highly varicose arborization that overlaps and extends well beyond the limits of the dendritic field of the cell of origin. The axonal arborization is the densest of all the striatal neurons (Fig. 8.1B). A subset of PV+ interneurons exhibits a more extended dendritic arborization and somata well in excess of 20 μm in diameter (Kawaguchi, 1993; Koós and Tepper, 1999; Tepper and Bolam, 2004). The proportion of striatal neurons in rat that are PV+ interneurons is 0.7% based on unbiased stereological cell counting (Rymar et al., 2004) and the neurons exhibit a dorsal to ventral and medial to lateral gradient of expression (Luk and Sadikot, 2001).

B. Intrinsic Membrane Properties

PV+ interneurons recorded *in vitro* in juvenile rats have the lowest input resistance of all striatal GABAergic interneurons ($86 \pm 38 \text{ M}\Omega$). These interneurons are hyperpolarized (resting membrane potential $\sim -80 \text{ mV}$) and display no spontaneous activity at rest. In a seminal study, of 11 neurons with these electrophysiological characteristics, 10 were immunopositive for PV and termed FSIs due to their suprathreshold electrophysiological properties (Kawaguchi, 1993). Subsequent experiments in slices from older rats revealed FSIs with essentially identical properties including a nearly linear IV response, low input resistance, hyperpolarized resting membrane potential and narrow action potentials with a rapid, large amplitude, and brief duration spike afterhyperpolarization (Bracci et al., 2002, 2003; Koós and Tepper, 1999, 2002; Taverna et al., 2007) (Fig. 8.1C).

When depolarized FSIs exhibit intrinsic membrane potential oscillation in the gamma frequency range that arises from the differences in the kinetics of voltage-gated channels, which may be important for processing synaptic inputs, as discussed later (Beatty et al., 2015).

Striatal FSIs form gap junctions with other FSIs (Kita, 1993; Kita et al., 1990). In one study, the coupling ratio ranged between 3% and 20%, and although the coupling was not strong enough to induce spiking *per se*, it was sufficient to synchronize depolarization-induced spiking in electrically coupled neurons such that the variability between spikes in the two neurons, when they did occur, was extremely small. This suggests that groups of FSIs may form an inhibitory syncytium capable of exerting powerful and synchronous inhibitory control over spike timing in a large number of MSNs, thereby influencing the temporal relationship of their spike trains leading to the formation of behaviorally relevant functional units (Koós and Tepper, 1999; but see Berke, 2008).

Electrotonic coupling with similar properties has been observed between pairs of FSIs in cortex and hippocampus (Freund and Buzsáki, 1996; Galarreta and Hestrin, 1999), although the highest coupling ratios in the cortical interneurons appear larger than in striatum, but this could be an artifact of the relatively small striatal sample size.

C. Firing Characteristics

FSIs have the shortest duration action potentials of all striatal neurons ($0.29 \pm 0.04 \text{ ms}$ at half amplitude), a rapid ($1.3 \pm 0.27 \text{ ms}$ time to peak) and brief spike afterhyperpolarization. One of the most characteristic properties of striatal FSIs is a nonlinear spiking

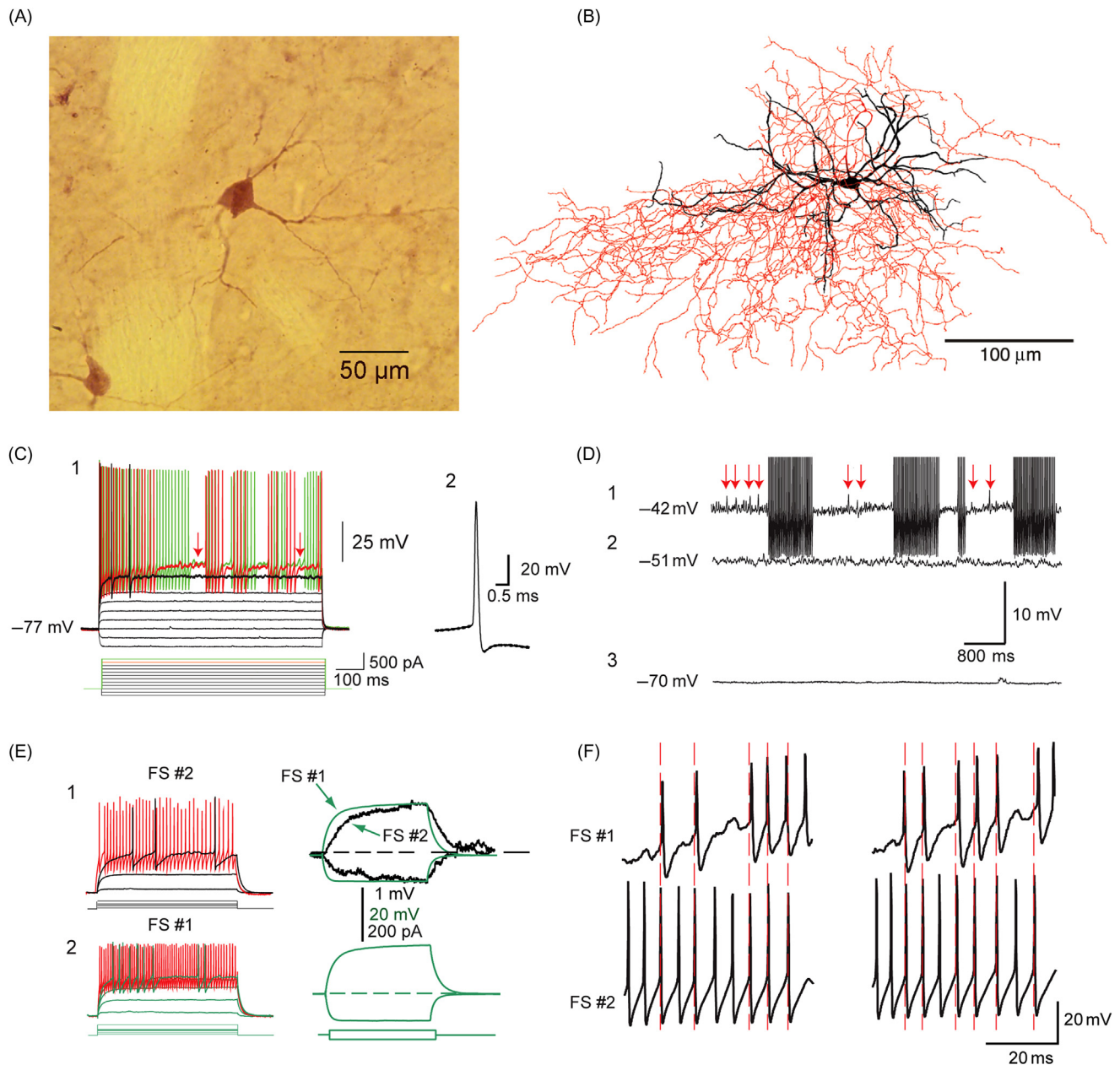


FIGURE 8.1 Striatal parvalbumin-positive (PV+) FSIs. (A) Typical morphology of an immunocytochemically labeled striatal GABAergic PV+ interneuron. (B) Drawing tube reconstruction of a biocytin-labeled rat striatal FSI that was presynaptic to a spiny projection neuron (not shown). Note the extremely dense axonal arborization (red) that extends beyond the simple, aspiny and compact dendritic arbor (black). (C1) Typical response of mouse striatal FSI to intracellular injection of current pulses. Note the low input resistance, the linear IV relation, and the characteristic nonlinear current-spiking relation where the minimum suprathreshold stimulus elicits a short burst of 3 spikes (black trace), whereas slightly larger current injection elicits a 120 ms burst of nonaccommodating spikes followed by a silent period followed by intermittent spiking (green trace) and a slightly larger current injection evokes longer periods of intermittent spiking. Sufficiently greater current injection elicits sustained firing in excess of 200 spikes/s (not shown). (C2) Note extremely narrow action potential and deep and rapid onset spike afterhyperpolarization. (D) Striatal FSIs are silent at rest (3). As they are depolarized, small subthreshold membrane oscillations occur (2) that eventually give rise to intermittent spiking (red arrows in 1). (E) Left two panels show a pair of FSIs that are electrotonically coupled. Intracellular current pulses injected into FS #1 (right lower panel) induces smaller, electrotonic responses in FS #2 (upper right, black traces) distorted by the membrane capacitance of the intervening dendrites. (F) Spiking induced by intracellular depolarization in a pair of electrotonically coupled FSIs is nearly synchronous due to the effects of the coupling. FS, fast spiking. Source: Figure modified from Koós, T., Tepper, J.M., 1999. Inhibitory control of neostriatal projection neurons by GABAergic interneurons. *Nat. Neurosci.* 2, 467–472.

response to intracellular depolarization. Low-amplitude stimuli of increasing strength produce only passive depolarizing responses but at a certain level, a tiny increase in stimulus strength results in the appearance of short bursts of spikes interrupted by periods of no spiking (Kawaguchi, 1993; Koós and Tepper, 1999, 2002; Kubota and Kawaguchi, 2000; Narushima et al., 2006; Sciamanna and Wilson, 2011). Stronger depolarizing pulses in striatal FSIs elicit high, sustained firing rates (> 200 spikes/s) with little spike frequency adaptation (Koós and Tepper, 1999, 2002; Plotkin et al., 2005; Sciamanna and Wilson, 2011) (Fig. 8.1C). The firing pattern of FSIs is somewhat unusual in that they cannot fire at arbitrarily low frequencies, and at rheobase fire a spike doublet with an average interspike interval (ISI) corresponding to about 44 spikes/s. Both the resonance and the stuttering firing pattern were unaffected by blocking Kv3 channels but both were abolished when Kv1 channels were blocked (Sciamanna and Wilson, 2011). Interestingly, the stuttering pattern is elicited in vitro by a steady depolarization, but not by a fluctuating input (Klaus et al., 2011), perhaps explaining why the stuttering pattern seen so often in vitro is not observed when animals are active in vivo (Berke, 2008, 2011; Berke et al., 2004).

During the nonspiking periods intercalated between episodic firing, prominent subthreshold gamma frequency, voltage-dependent membrane oscillations are observed (Beatty et al., 2015; Koós and Tepper, 1999, 2002; Sciamanna and Wilson, 2011; Taverna et al., 2007) (Fig. 8.1C1, D1). They are 2–3 mV in amplitude and exhibit a peak in power near 40 Hz (Bracci et al., 2003). The oscillations are able to induce episodes of firing and appear to be responsible for the stuttering, intermittent firing pattern of striatal FSIs. The oscillations and the intermittent firing pattern were resistant to blockade of Ca^{2+} channels, SK channels, or intracellular Ca^{2+} chelation. The oscillations were, however, completely eliminated by tetrodotoxin (TTX), indicating that they are due to an interaction between a persistent Na^{+} conductance and voltage-gated K^{+} conductances (Bracci et al., 2003). Whole cell recordings from striatal FSIs in slices from mice reveal that they express essentially identical properties to those described for rat FSIs (Centonze et al., 2003; Narushima et al., 2006; Sciamanna and Wilson, 2011; but see Freiman et al., 2006).

These electrophysiological characteristics are very similar to those of PV-expressing FSIs of adult mouse neocortex (Galaretta and Hestrin, 1999, 2001, 2002) and hippocampal basket cells (Freund and Buzsáki, 1996). The short-duration action potential, lack of spike frequency adaptation, and large spike afterhyperpolarizations are likely related to the expression of Kv3.1, a slowly inactivating delayed rectifier channel that

exhibits rapid activation and deactivation kinetics, and that is selectively expressed in striatum in FSIs (Lenz et al., 1994; Rudy and McBain, 2001).

D. Afferents and Efferents

PV+ interneurons receive a substantial monosynaptic input from the cortex, but in contrast to MSNs, which receive only one or two synapses from each individual cortical afferent (Kincaid et al., 1998), single cortical axons make multiple contacts with PV+ interneurons (Ramanathan et al., 2002). This may account, in part, for the greater responsiveness of PV+ interneurons to cortical stimulation (Parthasarathy and Graybiel, 1997) compared to MSNs (Mallet et al., 2005). In contrast to this powerful cortical input, FSIs receive few synaptic inputs from thalamus (Kita, 1993).

FSIs also receive GABAergic input from at least two different neuron populations in the external segment of the globus pallidus (GPe), PV+ (Bevan et al., 1998), and PV- (Mallet et al., 2012) neurons (see chapter: Organization of the Globus Pallidus), as well as cholinergic input, presumably from striatal cholinergic interneurons (ChIs) (Chang and Kita, 1992) (see chapter: The Cholinergic Interneuron of the Striatum) and possibly from brainstem as well (Dautan et al., 2014). It is interesting to note that although bath or local application of cholinergic agonists produces a strong mecamylamine-sensitive nicotinic excitation (Koós and Tepper, 2002; Luo et al., 2013), local electrical stimulation or optogenetic activation of striatal ChIs (English et al., 2012; Koós and Tepper, 2002) fails to evoke a cholinergic synaptic response. Perhaps this indicates a significant contribution from extra-striatal sources (eg, Dautan et al., 2014). There is also dopaminergic input, presumably from substantia nigra pars compacta (Kubota et al., 1987).

By far the predominant target of the FSI is the MSN (Fig. 8.2) (see chapter: The Striatal Skeleton: Medium Spiny Projection Neurons and Their Lateral Connections) with about 50% of striatal PV+ boutons synapsing pericellularly, on the soma or proximal dendrites of MSNs (Bennett and Bolam, 1994; Kita, 1993). Other PV+ boutons (some of which likely originated in GPe) have been observed making synapses with spiny dendrites as well as with varicose dendrites (Kita, 1993) belonging to PV+ interneurons and NOS-immunoreactive, presumably “plateau-depolarization low-threshold spike” (PLTS) (see later) interneurons (Bevan et al., 1998).

E. Synaptic Connectivity

Inhibitory postsynaptic potentials (IPSPs) in MSNs resulting from spiking of FSIs were first reported by Plenz and Kitai (1998) in an organotypic coculture of

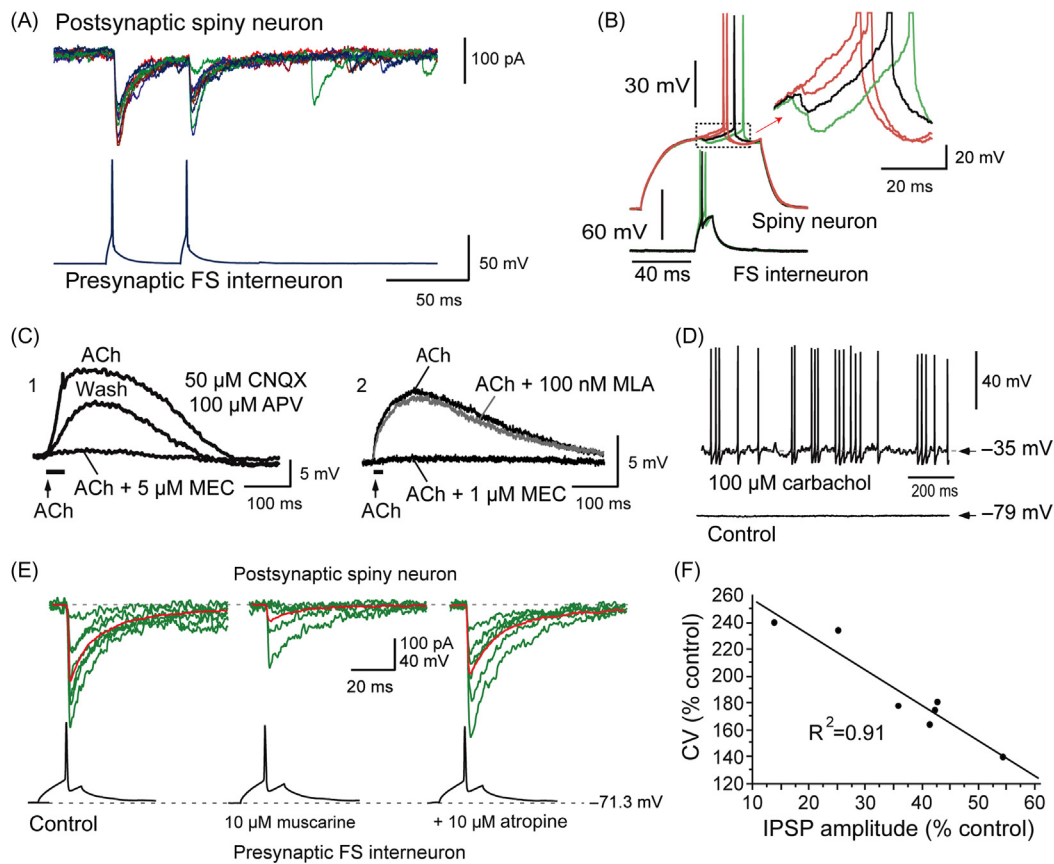


FIGURE 8.2 (A) Synaptic connections between FSIs and MSNs in rat exhibit large and variable amplitude and low failure rates. (B) Single IPSPs in FSIs elicit IPSPs in MSNs and delay the occurrence of spikes in MSNs evoked by intracellular current pulses (black trace). Presynaptic spike doublets evoked IPSPs that summate effectively and cause even greater delay in elicited MSN spikes (green trace). (C1) FSIs are depolarized by pressure application of ACh, which is completely blocked by mecamylamine (MEC). (C2) In contrast, ACh-induced depolarization is not blocked by the Type I nicotinic antagonist, MLA, indicating that the receptor is one of the nonsensitizing heteromeric subtypes. (D) Bath application of carbachol depolarizes an FSI and evokes intermittent spiking, effects that were sustained for the duration of the bath application. (E) Synaptic transmission between FSIs and MSNs is subject to powerful muscarinic inhibition. (F) Correlation between the mean amplitude depression and the CV of the depression shows that the effect is mediated presynaptically. *Source: Modified from Koós, T., Tepper, J.M., 2002. Dual cholinergic control of fast-spiking interneurons in the neostriatum. J. Neurosci. 22, 529–535.*

cortex, striatum, and substantia nigra. Soon after, paired whole cell recordings of FSIs and MSNs were obtained in striatal slices from adult rats (Koós and Tepper, 1999). These revealed unusually strong unitary IPSPs in the MSNs from single spikes in FSIs (Fig. 8.2). IPSPs were blocked completely by bath application of bicuculline indicating that the FSI–MSN synaptic response is mediated predominantly or exclusively by γ -aminobutyric acid-A (GABA_A) receptors. The synaptic connections were always unidirectional, from the FSI to the MSN, but never in the other direction, and were observed in approximately 25% of the paired recordings when the two cells were within 250 μ m of each other. The synaptic connection was remarkably reliable and for most pairs exhibited a failure rate of less than 1%.

Importantly, individual FSIs innervate MSNs of both direct and indirect striatal output pathways (Planert

et al., 2010) (see chapter: The Neuroanatomical Organization of the Basal Ganglia, for a description of these pathways), although a significant preference in probability of connectivity may exist for direct pathway MSNs (Gittis et al., 2010).

Early estimates of the convergence values of FSIs and MSNs were based on the known metrics of striatal cell counts (Oorschot, 1996) and the assumptions that all MSNs within an FSI's axonal arborization are innervated, and that FSIs comprise 5% of the cells in striatum. This yielded an upper limit of convergence of 27 FSIs per MSN. A lower limit was estimated by assuming that only 25% of the MSNs are innervated and only 3% of the striatal cells are FSIs and was calculated to be four FSIs per MSN (Koós and Tepper, 1999). However, in subsequent reports from our lab and others, the incidence of connectivity was

significantly higher, with a *lower* limit around 50% (Taverna et al., 2007; Tecuapetla et al., 2009). In terms of convergence, the increase in the lower limit of synaptic connectivity is offset by more accurate estimates of the number of PV+ neurons from stereological cell counts that suggest that the proportion of PV+ neurons in the rat striatum is actually only 0.7% (Rymar et al., 2004). This would give a lower limit of convergence of two FSIs per MSN and an upper limit of four FSIs per MSN.

Average unitary FSI–MSN IPSPs recorded in hyperpolarized MSNs were over 0.4 mV in amplitude, but when measured when the MSN was just subthreshold, averaged greater than 1 mV in amplitude. Temporal summation in response to bursts of 2–5 spikes in the FSI within 10–50 ms led to compound IPSPs that could be up to 7 mV in amplitude. The effectiveness of these IPSPs was evident by the ability of unitary IPSPs to significantly delay the timing of depolarization-evoked spikes in MSNs and, in the case of short bursts of presynaptic spikes, to completely block spiking in the MSN (Koós and Tepper 1999).

When compared to IPSPs arising from the local axon collaterals of MSNs (Czubayko and Plenz, 2002; Tecuapetla et al., 2009; Tepper et al., 2004; Tunstall et al., 2002) (see chapter: The Striatal Skeleton: Medium Spiny Projection Neurons and Their Lateral Connections), the feedforward FSI IPSP appeared significantly larger and had a significantly lower failure rate than the feedback collateral IPSP under a number of different experimental conditions (Gustafson et al., 2006; Guzman et al., 2003; Koós et al., 2004; Tecuapetla et al., 2005). Quantal analysis revealed that whereas individual FSI–MSN and MSN–MSN responses were in fact biophysically similar, the differences in average IPSP/C amplitude and failure rate could be attributable to a more proximal location and larger number of synapses formed by FSI inputs to MSNs than from collateral inputs from other MSNs (Koós et al., 2004). In addition to the powerful inhibition of MSNs, FSIs also make sparse and weak synaptic connections with PLTS interneurons, while completely avoiding ChIs (Szydłowski et al., 2013) and other GABAergic interneurons labeled in 5HT3aR mice (Faust, Assous, Koós and Tepper, unpublished). Thus, FSIs appear to target MSNs with great specificity.

F. In Vivo Recordings

In vivo recordings from unambiguously identified GABAergic interneurons are relatively rare. Intracellular recordings from a neuron identified post hoc by horseradish peroxidase staining as a likely PV+ FSI based on the large soma size and varicose dendritic arborization

exhibited excitatory postsynaptic potentials (EPSPs) in response to cortical stimulation. The EPSPs gave rise to short bursts of high-frequency spikes (Kita, 1993), as would be predicted from the in vitro responses of striatal FSIs.

Subsequently, extracellular single unit recording studies in vivo in anesthetized rats putatively identified FSIs on the basis of their short-duration action potentials and short, high-frequency (>300 Hz) bursts of 3–5 spikes, very similar to that reported by Kita (1993) in response to cortical stimulation (Mallet et al., 2006, 2005). These neurons exhibited spontaneous firing rates of around 0.5 spikes/s during slow wave sleep and 3.5 spikes/s at other times. When neurons with these characteristics were juxtacellularly stained with biocytin and then tested for PV immunoreactivity, all neurons tested were immunopositive for PV, thus unequivocally identifying them as PV+ FSIs (Mallet et al., 2005, 2006).

More recently, extracellular recordings in anesthetized rats followed by juxtacellular labeling and immunocytochemistry unambiguously identified PV+ FSIs in anesthetized rats (Sharott et al., 2012). These neurons exhibited highly variable rates of spontaneous activity that were not correlated with the power of cortical slow waves, but spiking was phase-locked to cortical gamma oscillations. Also of note, despite the wide range of firing rates, many of the neurons exhibited short bursts of action potentials with intervening silent periods, very similar to the stuttering pattern evoked by long depolarizing pulses in vitro.

FSIs were also shown to respond to bilateral and multimodal (tactile and visual) sensory stimulation in vivo (Reig and Silberberg, 2014; Sharott et al., 2012), as well as to direct cortical input from primary visual cortex (Khibnik et al., 2014).

Comparison of the responses of MSNs to those of FSIs following cortical stimulation showed the FSIs to be more responsive during periods of cortical desynchronization than during slow wave sleep, whereas the opposite was true for MSNs (Mallet et al., 2005). On average FSIs were more responsive to cortical stimulation than MSNs (Mallet et al., 2006), consistent with results from immediate-early gene expression experiments (Parthasarathy and Graybiel, 1997). Local application of picrotoxin increased the spiking of MSNs in response to cortical stimulation, particularly under conditions favoring the activity of FSI activity, suggesting that strong feedforward inhibition of MSNs by FSIs normally occurs in vivo as well as in vitro (Koós and Tepper, 1999, 2002; Mallet et al., 2005).

Presumed FSIs have also been identified in vivo in behaving rats. Tetrode recordings revealed a population of neurons that were spontaneously active with average firing rates of 5–30 spikes/s during waking that displayed narrow-duration waveforms and

high-frequency bursts during slow wave sleep, and an anatomical distribution very similar to that reported for PV+ FSIs (Berke, 2008; Berke et al., 2004). The presumed FSIs were more active when the animals were awake than during slow wave sleep, consistent with results from the anesthetized animals. These neurons were found to be entrained by high-voltage spindle activity that occurred principally while rats were immobile but interestingly, even nearby FSIs failed to exhibit correlated firing while rats were performing a radial maze task (Berke, 2008), suggesting that feedforward inhibition of individual MSNs may be comprised of inputs from FSIs with very different firing rates and/or behavioral correlates.

Importantly, FSIs synchronize their activity with low- and high-frequency gamma oscillations under specific conditions (Berke, 2011) possibly allowing brief, behaviorally specific entrainment of subpopulations of MSNs as well (Popescu et al., 2009).

FSI dysfunction has been implicated in certain neurological/psychiatric conditions in humans. Patients with Tourette syndrome (see chapter: Tourette Syndrome and Tic Disorders) have been reported to have reduced numbers of striatal FSIs (Kalanithi et al., 2005). In a rat model of hyperactivity and loss of impulse control, the genetically hypertensive rat, recordings of FSIs were encountered less frequently than in controls, and FSIs exhibited altered higher mean firing rate and altered burst firing, as well as a lack of sensitivity to amphetamine (Perk et al., 2015). Selective inactivation of FSIs leads to dyskinesias in mice (Gittis et al., 2011).

G. Pharmacology

Local or bath application of nicotinic cholinergic agonists in vitro depolarizes striatal FSIs by up to 40 mV, evoking episodes of irregular bursty firing in the normally silent neurons, thereby increasing feedforward inhibition of MSNs (Koós and Tepper, 2002; Luo et al., 2013). The cholinergic excitation persists during bath application of carbachol and is insensitive to high concentrations of the Type I nicotinic receptor antagonist, methyllycaconitine (MLA), but can be completely blocked by the nonspecific nicotinic antagonist, mecamylamine. This profile strongly suggests that the receptor responsible is one of the heteromeric, nondesensitizing nicotinic receptor subtypes (Alkondon and Albuquerque, 1993). Disfacilitation of FSIs as their nicotinic excitation is transiently reduced during the brief and stereotyped pause in striatal ChIs that accompanies behaviorally relevant stimuli (Aosaki et al., 1994) may play a role in relaying the pause to MSNs with high temporal fidelity (Koós and Tepper, 2002).

Acetylcholine (ACh) also acts through pirenzapine-sensitive muscarinic receptors located on axon terminals of striatal FSIs to inhibit GABA release presynaptically and reduce the feedforward inhibition of MSNs (Koós and Tepper, 2002). The balance of this dual cholinergic regulation of FSIs may depend on the behavioral state and the level of interneuronal activity with the direct excitatory nicotinic effects predominating when FSIs are relatively inactive during periods of cortical synchrony and the presynaptic inhibitory effects predominating during cortical desynchronization when FSIs are highly active.

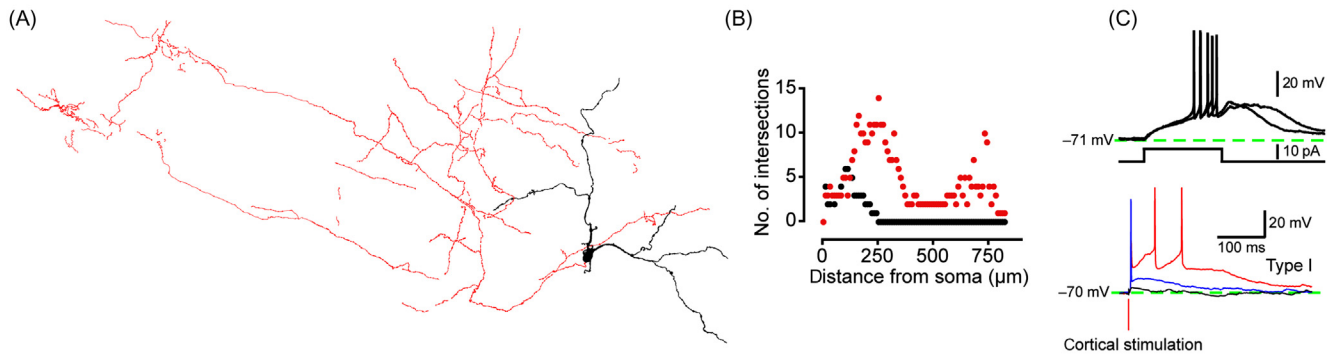
FSIs are also excited by dopamine (DA) (Bracci et al., 2002). The excitation is accompanied by a decrease in membrane conductance and, like nicotinic stimulation, is sufficient to generate spiking. These effects were blocked by the D1-like receptor antagonist SCH-23390 but not by the D2 receptor antagonist quinpirole, suggesting that they were mediated by a D1-like DA receptor. The excitation persisted in D1 knockout mice, indicating that it is mediated by D5 receptors that have been shown to be co-expressed with PV in striatal FSIs (Centonze et al., 2003). Interestingly, unlike direct pathway MSNs that express presynaptic D1 receptors on their axon terminals that facilitate GABA release (Misgeld et al., 2007), there is no presynaptic modulation of the FSI to MSN synapse by DA (Tecuapetla et al., 2009).

IV. NPY INTERNEURONS

A. Neurocytology

The discovery of SOM-immunoreactive interneurons in striatum was followed by demonstrations that SOM, NPY (Fig. 8.3), and Nicotinamide adenine dinucleotide phosphate (NADPH)-diaphorase/NOS were all co-expressed in the same neuronal population (Chesselet and Graybiel, 1986; Vincent and Johansson, 1983) and that these neurons were distinct from those that expressed PV or CR (Kubota et al., 1993). At first these interneurons did not appear to be GABAergic because unlike the other known striatal GABAergic interneurons, SOM-immunoreactive neurons did not appear to express GAD mRNA (Chesselet and Robbins, 1989) or immunoreactivity for GABA or GAD67 (Kubota et al., 1993). However, subsequent immunocytochemical labeling following colchicine treatment revealed that all NOS-reactive cells were strongly immunopositive for GAD67 (Kubota et al., 1993) and intracellular labeling followed by electron microscopic postembedding immunogold labeling for GABA or GAD showed there that synaptic boutons were strongly GABA/GAD immunopositive (Kubota and Kawaguchi, 2000).

NPY-PLTS



NPY-NGF

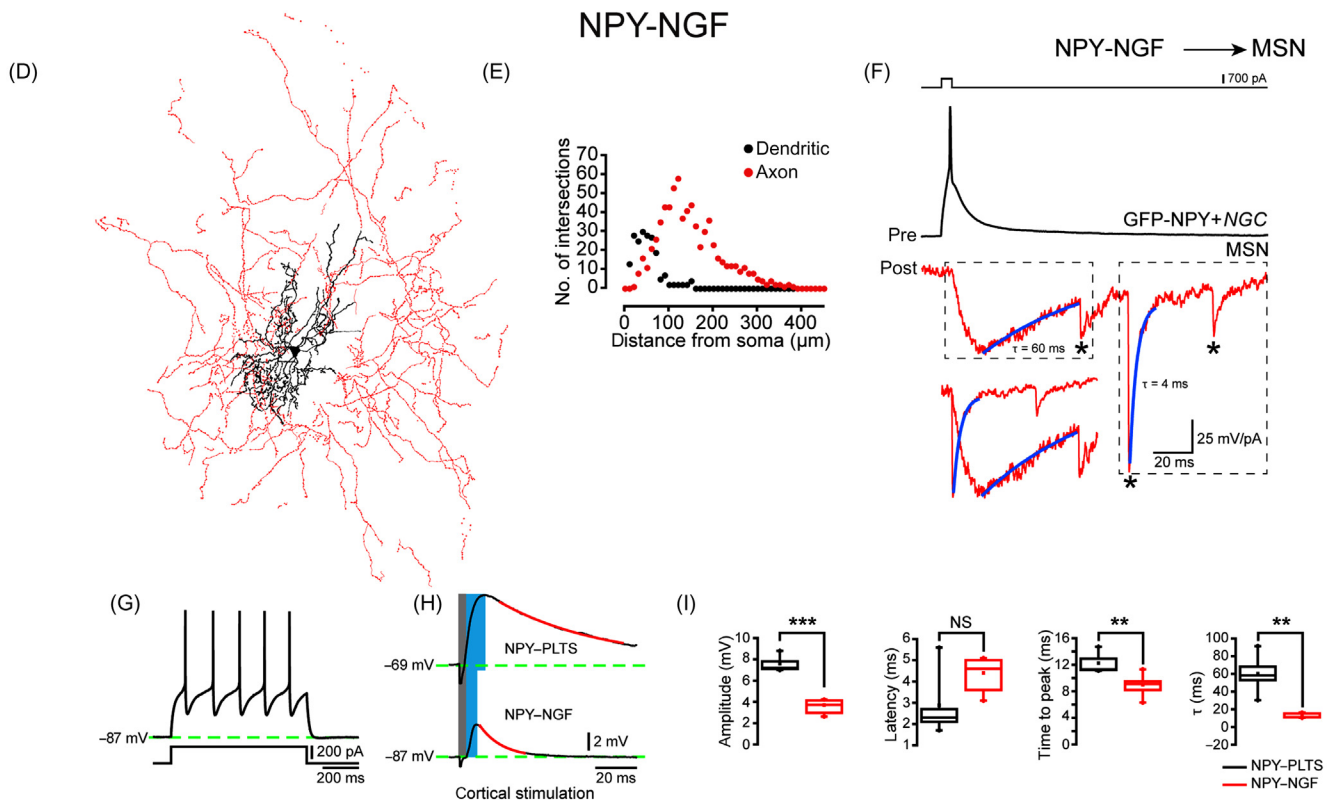


FIGURE 8.3 Striatal NPY interneurons. (A) Drawing tube reconstruction of an NPY-immunofluorescent interneuron electrophysiologically identified as an NPY-PLTS interneuron (axonal arbor in red, dendritic arbor in black). (B) Sholl plot of the drawing in (A) shows the very long and extended axonal field (red) that forms one large branched area at the periphery of the dendritic field (black) and another two several hundred micrometers away. (C, upper). Typical prolonged plateau potential in an NPY-PLTS interneuron that long outlasts the initiating depolarizing current injection. (C, lower). Responses to cortical stimuli of different intensities. Strong stimuli induce long-lasting plateau depolarizations evoking spikes. (D) Drawing tube reconstruction of a striatal NPY-immunofluorescent neuron electrophysiologically identified as an NPY-NGF interneuron. Note the highly branched, short, and densely packed dendritic tree (black), and the dense local axonal arborization (red) that overlaps and surrounds the dendritic field. (E) Sholl plot for this neuron. (F) Paired whole cell recordings between a presynaptic NPY-NGF interneuron and a postsynaptic MSN. Upper: Current-evoked spike in the NPY-NGF interneuron. Middle: Postsynaptic response in MSN is a $GABA_{A\text{slow}}$ IPSC (see text for details). Asterisks indicate spontaneous normal $GABA_{A\text{fast}}$ IPSCs. Lower: Overlay of normalized $GABA_{A\text{slow}}$ and $GABA_{A\text{fast}}$ IPSCs from middle trace. (G) Voltage response of NPY-NGF interneuron to intracellular depolarizing current pulse. Note deep and long-lasting spike AHPs. (H) Cortically evoked EPSPs in PLTS and NPY-NGF interneurons differ in (I) amplitude, latency, rise time, and decay time constant. *Source: Modified from Ibanez-Sandoval, O., Tecuapetla, F., Unal, B., Shah, F., Koós, T., Tepper, J.M., 2011. A novel functionally distinct subtype of striatal neuropeptide Y interneuron. J. Neurosci. 31, 16757–16769.*

SOM/NOS/NPY interneurons are medium sized. The neurons emit 2–5 thick, rapidly tapering aspiny primary dendrites that branch within 50 μm of the cell body, become varicose, and give rise to a relatively simple and unbranched dendritic arborization up to 600 μm in diameter (Aoki and Pickel, 1988; Kawaguchi, 1993; Vincent and Johansson, 1983; Vincent et al., 1983). The axonal arborization of SOM/NOS/NPY interneurons is the sparsest of any striatal neuron and is also the most extended, with unbranched axons tending to course in straight lines for up to 1 mm. Some of these neurons appeared to give rise to two main axons (Ibáñez-Sandoval et al., 2011; Kawaguchi, 1993; Tepper et al., 2010) (Fig. 8.3).

Unbiased stereological counts of rat striatal neurons immunostained for SOM (21,300) and NPY (14,355) differ (Rymar et al., 2004), consistent with the results of a double and triple labeling study that showed that only about 80% of SOM neurons also expressed NPY and that only 73% of neurons immunoreactive for SOM, NOS, NADPH-diaphorase, or NPY expressed all four peptides (Figueredo-Cardenas et al., 1996). Therefore the proportion of striatal neurons comprised of SOM/NOS/NPY cells would be somewhere between 0.55% and 0.8%. There is at least one case in which different combinations of co-expression of SOM, NOS, NADPH-diaphorase, and NPY are associated with different electrophysiological and morphological phenotypes (see later).

B. Intrinsic Membrane Properties

The SOM/NOS/NPY interneurons were another of the striatal GABAergic interneurons first described by Kawaguchi in brain slices from young rats (Kawaguchi, 1993). These cells were initially distinguished from MSNs and the other GABAergic interneurons by the presence of a low-threshold Ca^{2+} spike (*LTS*) that could be elicited by intracellular depolarization or synaptic stimulation delivered at the resting membrane potential, and by the expression of long-lasting depolarizing *plateau potentials* (*P*) that occurred following depolarizing current injections, sufficiently strong excitatory synaptic stimulation, or as a rebound upon cessation of a hyperpolarizing current injection. These neurons were thus termed PLTS interneurons (Kawaguchi, 1993) (Fig. 8.3). PLTS cells were further characterized by a high input resistance ($744 \pm 51 \text{ M}\Omega$), a relatively depolarized resting membrane potential ($-63 \pm 1 \text{ mV}$), and relatively long-duration action potentials ($1.3 \pm 0.05 \text{ ms}$) at half amplitude (Centonze et al., 2002; Kawaguchi et al., 1995; Kubota and Kawaguchi, 2000; Partridge et al., 2009; all numbers reported from mouse PLTS neurons from Ibáñez-Sandoval et al., 2011).

Although the original description of striatal PLTS interneurons in rat slices did not mention spontaneous activity (Kawaguchi, 1993), more recent reports in mouse slices indicate that the majority (up to 91%) of PLTS interneurons are spontaneously active in vitro (Beatty et al., 2012; Dehorter et al., 2009; Ibáñez-Sandoval et al., 2011; Partridge et al., 2009). Spiking is autonomous, not requiring any synaptic input (Beatty et al., 2012). Spiking in PLTS interneurons shows phase locking to a range of frequencies but is most sensitive (peak-spiking resonance) in the beta (10–20 Hz) frequency range, another characteristic that distinguishes them functionally from FSIs (Beatty et al., 2015).

C. Afferents and Efferents

Striatal PLTS neurons receive a monosynaptic excitatory input from the cortex that can evoke both spikes and long-lasting plateau potentials (Ibáñez-Sandoval et al., 2011; Kawaguchi, 1993) (Fig. 8.3). They also receive a dopaminergic innervation, presumably from the substantia nigra (Kubota et al., 1988; Li et al., 2002) and are also targeted by afferents from GPe (Bevan et al., 1998; Mallet et al., 2012). A recent optogenetic study also showed a very sparse (1/5 neurons) GABAergic input from FSIs (Szydlowski et al., 2013). Like FSIs, PLTS interneurons are not activated by optogenetic activation of striatal ChIs (English et al., 2012).

D. Synaptic Connectivity

There are relatively few recordings of synaptically connected PLTS interneurons and MSNs (Gittis et al., 2010; Ibáñez-Sandoval et al., 2011). The first study showed an extremely low (2/60; 3%) probability of PLTS interneurons evoking an IPSP on a nearby MSN in “blind” recordings of MSNs. However, the axonal arborization of most PLTS interneurons is very sparse and extends far from the soma (Gittis et al., 2010; Ibáñez-Sandoval et al., 2011; Kawaguchi, 1993). If one fills the PLTS interneuron with Alexa 594 to visualize the axonal field and then attempts to patch MSNs only in that field, the connection probability rises to 3/21 or 14% (Ibáñez-Sandoval et al., 2011), which is about the same one-way probability of synaptic connection between MSNs (Koós et al., 2004; Tecuapetla et al., 2009; Tunstall et al., 2002). These inhibitory postsynaptic currents (IPSCs) exhibited the kinetics of standard fast GABA_A -mediated IPSCs in striatum, with a rise time of $1.0 \pm 0.1 \text{ ms}$ and a decay time constant of $10.3 \pm 1.2 \text{ ms}$ (Ibáñez-Sandoval et al., 2011).

PLTS interneurons respond to modest cortical stimulation with EPSPs/EPSCs (excitatory postsynaptic currents). Slightly stronger stimulation leads to the

evocation of a long-lasting depolarizing plateau potential up to several hundred ms in duration upon which ride one or more normal action potentials (Ibáñez-Sandoval et al., 2011; Kawaguchi, 1993).

E. Pharmacology

PLTS interneurons are depolarized by bath application of DA, an effect that is blocked by the D1-like antagonist, SCH-23390. The depolarization is sufficient to trigger spiking and is associated with a decrease in membrane conductance (Centonze et al., 2002). More than 75% of striatal SOM+ neurons are also immunoreactive for the D5 receptor (Rivera et al., 2002), whereas most show no D1 mRNA expression and those that do express only low mRNA levels (Le Moine et al., 1991). Thus, like the PV+ interneurons, the excitatory effects of DA on PLTS interneurons are mediated by D5 receptors. Chronic depletion of DA causes PLTS neurons to switch to a rhythmic bursting pattern (DeHortor et al., 2009).

PLTS interneurons also exhibit a nicotinic EPSC and enhanced firing in response to bath application of cholinergic agonists (Luo et al., 2013).

V. NPY-NEUROGLIAFORM INTERNEURONS

A. Neurocytology

Following the introduction of a BAC transgenic mouse line in which the yellow fluorescent protein (YFP) reporter was controlled by NPY regulatory elements, a second type of striatal NPY interneuron was discovered (Ibáñez-Sandoval et al., 2011). Under standard epifluorescence illumination, two distinct types of medium-sized enhanced yellow fluorescent protein (EYFP)-NPY neurons were readily apparent. The more common type, comprising about 75% of the population, exhibited moderately bright fluorescence and emitted from 1 to 3 long, unbranched, aspiny primary dendrites. Subsequent immunocytochemistry revealed that these neurons co-expressed SOM and NOS, and their electrophysiological properties and biocytin reconstructions revealed that they were identical to the PLTS described above.

However, the second NPY cell population was several times brighter under the same illumination and issued from 5 to 9 short, aspiny primary dendrites that rapidly branched forming an extremely dense but compact dendritic field (Fig. 8.3). Although these interneurons expressed NPY, none of them co-expressed either SOM or NOS. The dendritic field was extremely dense and compact, fairly symmetrical and usually

less than 200 μm in diameter, and the axonal arborization was also dense and extending well over 400 μm in diameter. On the bases of these neurocytological properties and their great similarity to previously reported cortical and hippocampal neurogliaform (NGF) interneurons, we termed this second population of striatal NPY cells striatal NPY-NGF interneurons (Ibáñez-Sandoval et al., 2011; Luo et al., 2013).

B. Intrinsic Membrane Properties

NPY-NGF interneurons exhibited intrinsic electrophysiological properties that were distinct from any other previously described striatal neurons. Unlike the NPY-PLTS neurons, NPY-NGF interneurons were very hyperpolarized in vitro (-88 ± 1 mV vs -63 ± 1 mV) and did not fire spontaneously. Their input resistance (142 ± 13 M Ω) was much lower than that of PLTS interneurons (744 ± 51 M Ω), and they did not exhibit either the LTS or the long-lasting plateau potentials of the PLTS interneurons in response to current injection. Rather, voltage responses to varying current injections were somewhat similar to those of MSNs, including significant inward rectification, differing principally by their greater input resistance and a very deep and long-duration spike afterhyperpolarization (Ibáñez-Sandoval et al., 2011; Luo et al., 2013). Pairs of NPY-NGF interneurons are also electrotonically coupled (English et al., 2012).

C. Afferents and Efferents

NPY-NGF interneurons receive glutamatergic inputs from cortex. However, unlike PLTS or FSIs, even the strongest cortical stimulation evokes only subthreshold EPSPs (Ibáñez-Sandoval et al., 2011). In contrast, optogenetic stimulation following injection of CAMK II promoter-based AAV coding for channelrhodopsin2 (ChR2)-YFP into the region of the centromedian-parafascicular nuclei of the thalamus depolarizes NPY-NGF interneurons from rest and causes them to fire action potentials (Assous and Tepper, unpublished).

In addition, there is a powerful nicotinic cholinergic input that arises from striatal ChIs (an additional contribution from recently discovered brainstem cholinergic afferents from the pedunculo-pontine and lateral dorsal tegmental nuclei cannot be excluded (Dautan et al., 2014)). Activation of striatal cholinergic axons optogenetically or by intracellular stimulation of striatal cholinergic neurons activates a disynaptic pathway mediated through the activation of NPY-NGF interneurons that elicits a strong inhibition of MSNs (English et al., 2012).

NPY-NGF interneurons make powerful GABAergic synapses onto MSNs, with an 86% (25/29) connection

probability in paired recordings (Ibáñez-Sandoval et al., 2011). The resulting IPSC is mediated by GABA_A receptors, but displays unusually slow kinetics, with a rise time of 10 ± 1 ms and a decay time constant of 123 ± 42 ms, about one order of magnitude slower than PLTS-elicited and other GABA_A IPSCs reported in striatum (English et al., 2012; Ibáñez-Sandoval et al., 2011), but similar to that of GABA_A slow reported in cortex and hippocampus (Fuentealba et al., 2008; Price et al., 2005). This GABA_A slow synaptic current is in part responsible for a powerful inhibition of MSNs that can be triggered by rebound excitation of striatal ChIs and thus may contribute to the interruption and reorientation of ongoing behavior when salient stimuli are encountered (English et al., 2012).

D. Pharmacology

The nicotinic receptor expressed by the NPY-NGF interneuron is sensitive to low concentrations of dihydro- β -erythroidine (Dh β E) (English et al., 2012; Luo et al., 2013) suggesting that they express β 2 subunit containing nicotinic receptors, most likely α 2 β 2.

VI. STRIATAL TYROSINE HYDROXYLASE INTERNEURONS

Originally identified in the striatum of adult monkeys by tyrosine hydroxylase (TH) immunocytochemistry (Dubach et al., 1987), striatal TH-immunoreactive (TH+) neurons have subsequently been reported in a number of other species including rat (Tashiro et al., 1989; Meredith et al., 1999), mouse (Mao et al., 2001; Petroske et al., 2001), monkeys (Betarbet et al., 1997; Mazloom and Smith, 2006), and man (Cossette et al., 2005; Huot et al., 2007).

Using TH-Cre mice that express enhanced green fluorescence protein (EGFP) under the control of the TH endogenous regulatory mechanisms, we identified a relatively large population of EGFP-TH+ neurons (THINs) in mouse striatum (Ibanez-Sandoval et al., 2015, 2010; Unal et al., 2011, 2015) (Fig. 8.4). These neurons were classified on the basis of two- and three-dimensional clustering of passive and active electrophysiological properties into four different cell types that were clearly distinct from each other and from MSNs, ChIs, FSIs, or NPY GABAergic interneurons. Injection of fluorescent-labeled beads into substantia nigra and GPe failed to produce any retrograde labeling of the THINs, demonstrating that they are, in fact, striatal interneurons (Ibanez-Sandoval et al., 2010).

The most common THIN subtype, TH Type I interneurons, comprise 60–80% of all striatal THINs

(Ibanez-Sandoval et al., 2010, 2015; Unal et al., 2011, 2015). Type I THINs are characterized by a very strong spike frequency adaptation that leads to complete spike failure after 100 ms or so in response to moderately strong depolarizing current injections. Striatal neurons that are electrophysiologically and pharmacologically identical to Type I THINs have also been identified in wild-type mice (Luo et al., 2013), proving that these neurons are definitely not an artifact of the EGFP-TH transgenic mouse. Type II and III THINs are both types of FSIs and are rare, whereas Type IV THINs (~20% of the total) exhibit an LTS, but not the same type of prolonged plateau depolarizations that characterize the NOS/NPY PLTS neuron described by Kawaguchi and others (Kawaguchi, 1993; Kawaguchi et al., 1995).

Interest in striatal THINs was intensified after it was consistently reported that the number of these cells increased greatly following 6-hydroxydopamine (6-OHDA) or 1-methyl-4-phenyl-1,2,3,6-tetrahydropyridine (MPTP) lesions that destroyed the nigrostriatal DA innervation. Many assumed that striatal THINs were dopaminergic and might therefore serve as an intrinsic source of DA that could compensate for the loss of DA in experimental or idiopathic Parkinson's disease (eg, Betarbet et al., 1997; Cossette et al., 2005; Darmopil et al., 2008; Gittis and Kreitzer, 2012; Huot and Parent, 2007; Meredith et al., 1999; Porritt et al., 2000; Tande et al., 2006). However, we recently showed that none of the striatal THINs expressed immunoreactivity for DA, L-aromatic acid decarboxylase, the vesicular monoamine transporter 2 (VMAT2), or the DA transporter. Furthermore, in vitro voltammetry coupled with optogenetics showed that while DA could be readily evoked in striatum by optical stimulation following viral transduction of nigrostriatal DA neurons and axons with ChR2, optical stimulation after selective viral transduction of striatal THINs alone with ChR2 failed to produce any measurable DA release, even after preloading with L-DOPA and in the presence of DA uptake blockers (Xenias et al., 2015). Thus striatal THINs are not dopaminergic but rather a class of monoenzymatic neurons (Ugrumov, 2009) that express TH, but none of the other enzymes necessary for the synthesis or synaptic release of DA.

When EGFP-TH mice were unilaterally injected with 6-OHDA, there was a statistically significant increase in the number of striatal THINs measured with unbiased stereological techniques following complete destruction of ipsilateral nigrostriatal neurons (Unal et al., 2015). However, this increase was very small and transient, peaking at 130% of control 7 days post lesion before returning to normal between 14 and 28 days later. While the increase in the number of THINs was small, it was also observed that the expression of TH

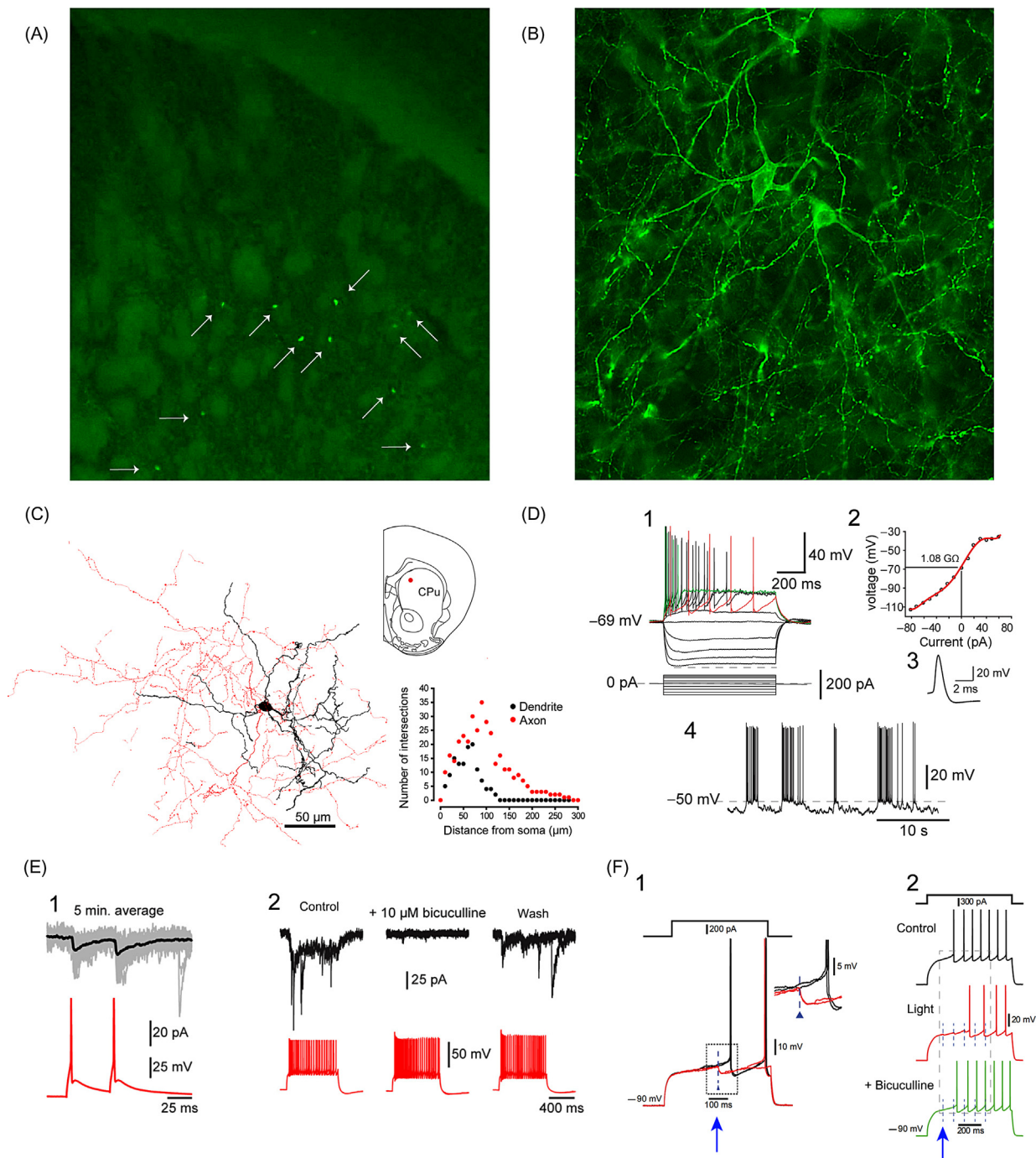


FIGURE 8.4 Striatal THINs. (A) Low-magnification fluorescence photomicrograph of a 60 μm section through the striatum of a BAC transgenic mouse that expresses EGFP under the control of the TH promoter. Arrows point to EGFP+ THINs. (B) High magnification fluorescence micrograph of striatal THINs labeled following local injection of an AAV coding for ChR2-YFP in a TH-Cre mouse. Note density of processes in neuropil, all of which derive from striatal THINs. (C) Drawing tube reconstruction of a striatal Type I EGFP-TH+ neuron filled with biocytin after recording in vitro. Note the varicose dendrites (black) and axonal arborization (red). Insets show localization in striatum (CPu) (upper) and Sholl plot of quantifying dendritic and axonal arborization. (D1) Responses to depolarizing and hyperpolarizing current injections in a Type I EGFP-TH+ neuron. Extreme spike frequency adaptation leading to complete spike failure, the sag in response to hyperpolarizing current pulses, the high input resistance (D2) and wide-duration action potential (D3) are all characteristics of this, the most common of the striatal EGFP-TH+ neurons, as is spontaneous activity (D4). (E) Paired recordings between a presynaptic THIN (red) and a postsynaptic MSN (black). (E1) Averaged IPSPs (black trace; all responses shown in gray) in a synaptically connected MSN induced by repeated double pulse intracellular stimulation of a THIN (red). (E2) Spike trains induced in a THIN by current injection and bicuculline-sensitive GABA_A IPSCs in the connected MSN in voltage clamp. Note the short-term depression. (F) Current clamp recordings of an MSN following optogenetic stimulation (blue arrows) of ChR2 transduced THINs. (F1) Paired

protein in striatal THINs, as detected immunocytochemically, increased dramatically. We concluded that the reason that many previous studies reported large increases in the number of TH-immunopositive interneurons, while with our techniques the increase was quite modest, was that the BAC transgenic EGFP-TH mice, which contained multiple copies of the transgene (Gong et al., 2003), were much more sensitive reporters of TH gene activity than TH immunocytochemistry, and that the “newly induced” TH interneurons detected by others using TH immunocytochemistry were already detected in our control animals by the EGFP expression (Unal et al., 2015).

A. Afferents and Efferents

THINs are well integrated into the functional architecture of the striatum. Local stimulation elicits glutamatergic EPSPs and GABA_A IPSPs, and paired recordings show that the most common efferent targets are the MSNs (Fig. 8.4). Evoked spiking in striatal THINs produces potent, fast GABA_A IPSP/Cs in MSNs that are sufficient to significantly delay spikes evoked by intracellular depolarization. The IPSP/IPSCs are completely blocked by picrotoxin or bicuculline demonstrating that the THINs are also GABAergic (Ibanez-Sandoval et al., 2010) (Fig. 8.4).

THINs also receive monosynaptic glutamatergic cortical inputs as they respond to cortical stimulation with EPSPs that elicit spiking, both of which are blocked by bath application of 6-cyano-7-nitroquinoxaline-2,3-dione (CNQX) (Ibanez-Sandoval et al., 2010).

THINs are also strongly modulated by dopaminergic nigrostriatal afferents. The frequency of spontaneous EPSCs and IPSCs was significantly increased following 6-OHDA midbrain lesions of the nigrostriatal system in EGFP-TH mice. Interestingly, there was also a decrease in the time to peak of the spontaneous EPSCs following 6-OHDA lesions that was accompanied by an increase in the density of proximal spine-like protrusions (Unal et al., 2015). This suggests that, even though they are not dopaminergic (Xenias et al., 2015), striatal THINs might still play a compensatory role following experimental or idiopathic loss of nigrostriatal DA input, by increasing their output and thereby countering the hyperactivity that occurs in indirect pathway MSNs

under those conditions (Kita and Kita, 2011; Schultz and Ungerstedt, 1978; Unal et al., 2015).

B. Synaptic Connectivity

THINs make bicuculline-sensitive monosynaptic connections with MSNs. In the first set of studies (Ibáñez-Sandoval et al., 2010), in 5/34 or about 15% of the recorded pairs, spikes in the THIN led to a fast monosynaptic IPSP/C in the postsynaptic MSN. These ranged in amplitude from 9 to 12 pA and from 0.7 to 1.8 mV, and were able to block or completely abolish evoked spikes in the MSNs, depending on the timing of the IPSP relative to the spike in the MSN.

Interestingly, in 6 out of 18 pairs tested, current-evoked spikes in an MSN were able to elicit IPSPs in Type I THINs. This was the first example reported of MSNs synapsing back onto a GABAergic interneuron, something that we never observed with synaptically connected pairs of MSNs and FSIs (Koós and Tepper, 1999).

In subsequent optogenetic experiments in slices from TH-Cre mice in which THINs were virally transduced to express ChR2-YFP (Xenias et al., 2015), optical stimulation produced inhibition in 100% of the 18 MSNs recorded. The optogenetic synchronous activation of large populations of striatal THINs produced IPSCs that were roughly three times the amplitude of those observed in paired recordings, suggesting an upper limit of convergence of TH interneurons onto MSNs of about 3:1 (Xenias et al., 2015). Since direct and indirect pathway MSNs are about equally distributed in the striatum, this indicates that striatal THINs exert a widespread GABAergic inhibition throughout the striatum onto both direct and indirect pathway neurons, and therefore play an important role in both feedforward and feedback inhibition in striatum.

EGFP-TH interneurons also elicit conventional fast IPSCs in both postsynaptic FSIs and PLTS interneurons (Assous, Faust, Koós and Tepper, unpublished).

C. Pharmacology

There have only been two studies describing the pharmacology of striatal THINs (Luo et al., 2013; Ibáñez-Sandoval et al., 2015). All striatal THINs tested (Types I, II, and IV) responded to DA, SKF-38391 (a

recordings showing IPSP and complete blockade (red trace) of depolarization-induced spikes (black trace) in a synaptically connected MSN upon optogenetic activation of presynaptic THIN (blue arrow). Inset shows IPSP and spike failures at higher gain. (F2) Optogenetic activation (blue arrow and dashed lines) decreases spiking of an MSN in response to a 500 ms depolarizing current injection. Source: (For C): Modified from Ibanez-Sandoval, O., Xenias, H.S., Tepper, J.M., Koós, T., 2015. Dopaminergic and cholinergic modulation of striatal tyrosine hydroxylase interneurons. *Neuropharmacology* 95, 468–476. (For D, E): Modified from Ibanez-Sandoval, O., Tecuapetla, F., Unal, B., Shah, F., Koós, T., Tepper, J.M., 2010. Electrophysiological and morphological characteristics and synaptic connectivity of tyrosine hydroxylase-expressing neurons in adult mouse striatum. *J. Neurosci.* 30, 6999–7016. (For F): Modified from Xenias, H., Ibáñez-Sandoval, O., Koós, T., Tepper, J.M., 2015. Are striatal tyrosine hydroxylase interneurons dopaminergic? *J. Neurosci.* 35, 6584–6599.

selective D1-class agonist), or amphetamine with the appearance of, or an increase in duration of depolarization-induced plateau potentials that are characteristics of these neurons (Ibáñez-Sandoval et al., 2015; Unal et al., 2015). The amphetamine response, as well as changes in striatal THIN morphology, physiology, and TH levels following loss of endogenous DA (Unal et al., 2015), suggests that these interneurons are sensitive to endogenous levels of DA in striatum. Consistent with this idea, DA immunocytochemistry reveals DA-positive puncta surrounding THINs in striatum that disappear following 6-OHDA treatment (Xenias et al., 2015).

Spontaneous and DA-induced plateau potentials were eliminated in Na^+ -free buffer and blocked by the L-calcium channel antagonist, nimodipine. These characteristics, as well as complete blockade by flufenamic acid, strongly suggest that the underlying current that is manifested or enhanced by D1/D5 agonists is I_{CAN} . I_{CAN} is mediated by a melastatin-related transient receptor potential channel (TRPM), most likely a TRPM2 channel. These channels are expressed mostly in brain, are regulated by calcium, are nonselective permeable to monovalent cations and calcium, and are blocked by flufenamic acid (Fleig and Penner, 2004; Hill et al., 2004; Lee and Tepper, 2007; Lee et al., 2013).

Striatal THINs depolarize in response to local application of the nicotinic agonist, carbachol. This depolarization is unaffected by MLA or Dh β E, but is abolished by mecamylamine, a selective Type III nicotinic receptor antagonist (Ibáñez-Sandoval et al., 2015; Luo et al., 2013) and is mimicked by cytisine, a selective $\alpha 3\beta 4$ nicotinic agonist (Luo et al., 2013). Thus the nicotinic receptor on striatal THINs differs from that expressed by striatal FSIs and NPY-NGF interneurons (English et al., 2012; Koós and Tepper, 2002).

VII. FAST ADAPTING INTERNEURONS

In the mouse cortex, several different subtypes of GABAergic interneurons express the 5HT3a receptor subunit (Lee et al., 2010; Rudy et al., 2011). In the transgenic 5HT3a-EGFP mouse (Gerfen et al., 2013), these interneurons are readily visible and accessible for in vitro recording and staining in the striatum as well (Munoz-Manchado et al., 2014). Using a different but related transgenic mouse that expressed Cre instead of EGFP under control of the 5HT3a receptor promoter, we found a novel interneuron that was immunonegative for PV, TH, or NPY and comprised a single population with homogeneous morphological and electrophysiological properties and synaptic connections not previously reported for striatal interneurons. These were termed striatal fast adapting interneurons (FAIs; Faust et al., 2015) (Fig. 8.5)

A. Neurocytology

In a limited sample of electrophysiologically identified, biocytin-filled cells, FAIs were medium-sized isotropic multipolar neurons with 3–5 primary varicose dendrites that extended over an area approximately 300 μm in diameter. The axonal field overlapped and extended beyond the dendritic arbor and was comprised of thin, highly branched varicose and aspiny dendrites. These characteristics share significant overlap with many other striatal GABAergic interneuron subtypes, with the notable exceptions of NPY-PLTS and NPY-NGF interneurons (see earlier).

B. Afferents, Efferents, and Synaptic Connectivity

Much of the afferent and efferent connectivity of FAIs remains to be determined. However, paired recordings between FAIs and MSNs showed that spikes in FAIs evoked fast bicuculline-sensitive GABA_A IPSCs in MSNs. This synaptic connection was notable for its high success probability (50% in 11 out of 22 connection tested) and for the remarkably strong short-term facilitation of the MSN IPSC in response to brief trains of presynaptic FAI action potentials (Faust et al., 2015). This is in contrast to all other inhibitory GABAergic synapses in striatum previously observed that display short-term depression (Gittis et al., 2010; Koós et al., 2004; Taverna et al., 2007; Tecuapetla et al., 2007).

C. Pharmacology

Following optogenetic activation of striatal ChIs in choline acetyltransferase (ChAT)-ChR2 \times Htr3a-Cre double transgenic mice, the FAIs receive a powerful suprathreshold nicotinic cholinergic input in vitro. The pharmacology of this input was observed to be heterogeneous throughout the population, with some neurons being inhibited by the Type II nicotinic receptor antagonist, DH β E, and others inhibited by the Type III antagonist mecamylamine. The nicotinic receptor-mediated activation of FAIs may constitute an important mechanism through which ChIs control the activity of projection neurons and perhaps the plasticity of their synaptic inputs when animals encounter reinforcing or otherwise salient stimuli.

VIII. CALRETININ INTERNEURONS

CR-expressing (CR+) interneurons (Fig. 8.6) are medium sized (12–20 μm in diameter). They issue a small number of smooth, aspiny dendrites that branch sparingly and taper into very thin processes (Bennett

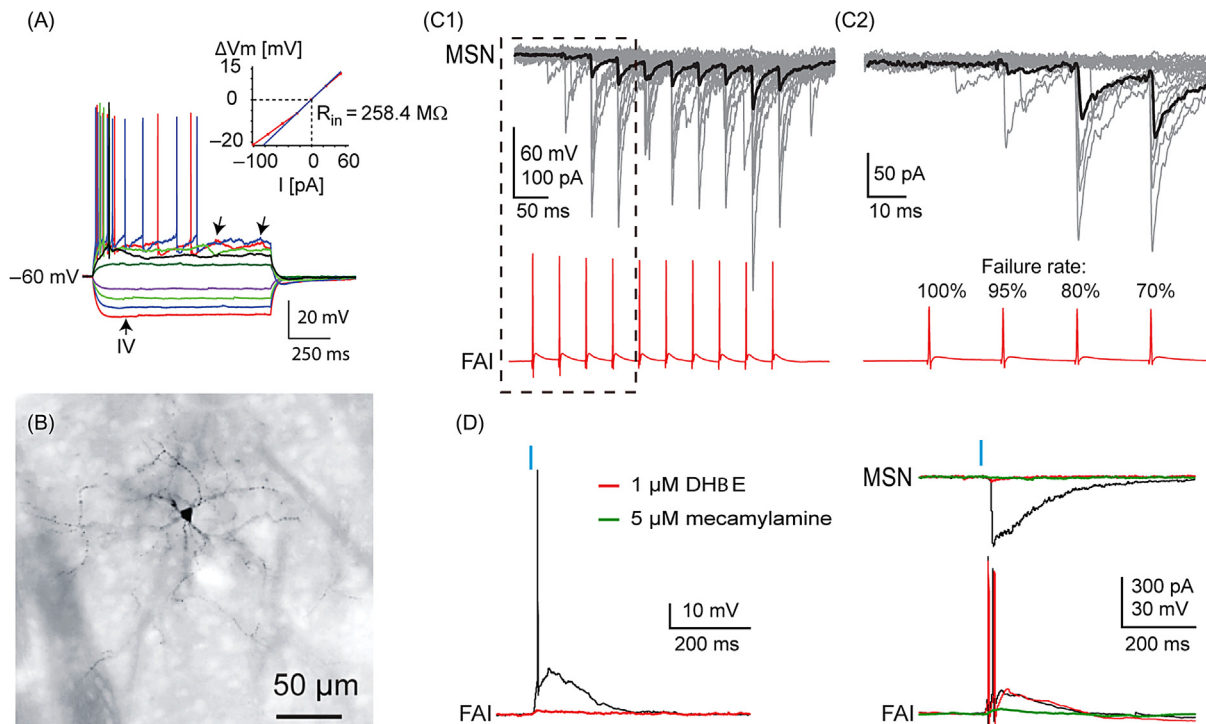


FIGURE 8.5 Electrophysiological and morphological properties of FAIs. (A) A typical FAI displays strong spike-frequency adaptation and a relatively depolarized resting membrane potential. Arrows indicate slow, irregular membrane potential fluctuations after spiking has completely adapted. Inset shows IV curve and input resistance. (B) Low-magnification photomicrograph of a biocytin-filled FAI reveals a medium-sized soma that gives rise to many highly varicose dendrites. (C1) The FAI–MSN synapse exhibits strong short-term facilitation to a 50 Hz presynaptic spike train. (C2) Expanded view of the first four stimuli in the train shown in C1 with the mean failure rates noted above each of the spikes in the train. Note that the failure to the first presynaptic spike is 100% in this pair. (D) Pharmacology of nicotinic input to FAIs. Left: Nicotinic EPSP and spike in response to optogenetic activation of ACh input (blue bar; 2 ms light pulse) in FAI. Following application of Type II nicotinic receptor antagonist, DHβE (1 μ M; red trace), the nicotinic response is abolished. Right: Nicotinic EPSP and spiking in response to optogenetic activation of ACh input (blue bar; 2 ms light pulse) in FAI (bottom) and simultaneously recorded IPSC in voltage clamp in MSN (top). Following application of DHβE (red traces), nicotinic-induced IPSC in MSN is abolished, but nicotinic excitation of FAI is unaffected. Following application of the nonspecific nicotinic antagonist, mecamylamine (5 μ M; green traces), the nicotinic EPSP in FAI is abolished. Source: Modified from Faust, T.W., Assous, M., Shah, F., Tepper, J.M., Koos, T., 2015. Novel fast adapting interneurons mediate cholinergic-induced fast GABA_A inhibitory postsynaptic currents in striatal spiny neurons. *Eur. J. Neurosci.* 42, 1764–1774.

and Bolam, 1993). All the anatomical information we have is from immunocytochemical studies as there have been no recordings or biocytin labeling; so little is known about the detailed neurocytology of rat CR+ neurons. CR+ interneurons make up a similar proportion of neurons in the rodent striatum as the PV+, FSI, and SOM/NPY GABAergic interneurons, about 0.8% (Rymar et al., 2004). However, in primates including humans, the proportion of CR+ neurons is much greater and outnumbers that of PV+ and SOM/NPY interneurons by 3 or 4 to 1 (Wu and Parent, 2000). Furthermore, in the human striatum, there are four morphologically distinct types of neurons that express CR (Prensa et al., 1998).

Neonatal hypoxia results in the neurogenesis of striatal CR+ interneurons in rats that persists for at least 5 months after induction. Interestingly the neurogenesis appears limited to the CR+ interneurons since there is no neurogenesis of striatal neurons that express

markers for any of the other striatal interneurons or projection neurons (Yang et al., 2008).

Recent studies in our lab have also revealed at least three distinct morphologies of striatal interneurons that are immunoreactive for CR in mice and rats (Shah et al., 2012) (Fig. 8.6). These different subtypes appear to be heterogeneously distributed in mouse striatum, with the small, monopolar, and spiny Type I CR interneuron the predominant CR+ neuron in the rostro-dorsal regions of the striatum, while the more common Type I and II CR interneurons are distributed more uniformly in the middle and caudal striatal regions (Shah et al., 2012).

Almost nothing is known about the neurophysiology of the CR interneurons, although at least Type I has been shown to evoke GABAergic IPSCs on MSNs (Shah et al., 2012). There have been no other published recordings of these cells in vitro to date, and no way to identify them from in vivo recordings.

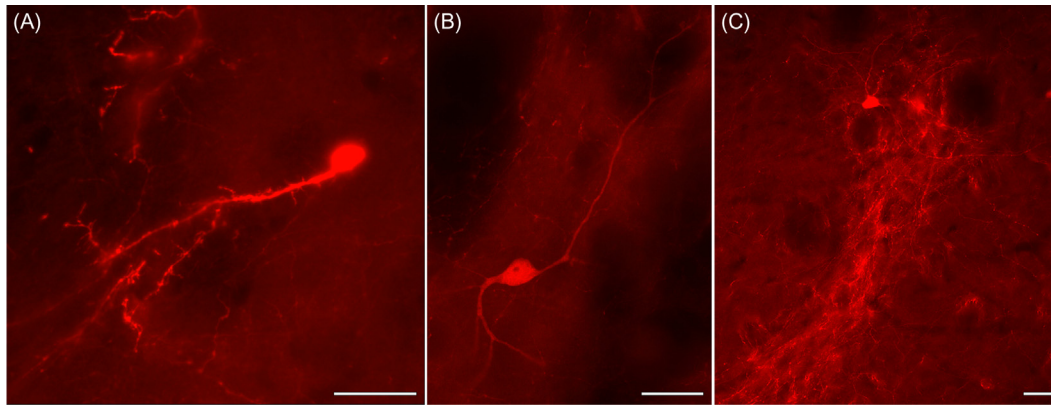


FIGURE 8.6 Striatal CR interneurons. (A) Example of a Type I, small, spiny unipolar CR-immunofluorescent interneuron. Type I CR interneurons are largely constrained to the dorsal anterior boundary of the striatum. (B) Example of a Type II, medium-sized CR-immunofluorescent interneuron that exhibits thick, aspiny, and sparsely branching dendrites. (C) Two Type III CR interneurons emit several thin, primary dendrites that issue slightly varicose higher order dendrites. Note the patch of intense CR immunofluorescent neuropil surrounding and ventral to the somata. Such patches were commonly observed around CR-immunofluorescent somata. Calibration bars are 25 μm .

IX. RECURRENT INTERNEURONS

In addition to the interneurons listed above, there is indirect evidence for the existence of at least one additional cell type, that we refer to as recurrent interneurons. Using *in vitro* slice recording experiments, Sullivan et al. (2008) have shown that GABAergic IPSCs can be elicited in ChIs using extracellular electrical stimulation that are dependent of the activation of Type II nicotinic receptors. IPSPs with similar pharmacological properties could also be triggered in a few instances with the activation of single ChIs. These responses were termed recurrent IPSCs reflecting the reciprocal relationship between the source(s) of GABA release and the ChIs. The same phenomenon was subsequently replicated using optogenetic activation of ChIs and extended with the demonstration that in slices obtained from mice recurrent inhibition can be elicited by activation of single ChIs with a significantly higher frequency, possibly reflecting more favorable preservation of circuits in this species.

The cellular mechanisms mediating these responses have not yet been determined with certainty. The observation that in a substantial number of cases, repeated cholinergic stimulation induces two or more IPSCs that vary from trial to trial in amplitude but exhibit relatively constant latencies strongly suggest that the IPSCs are elicited by the firing of a train of action potentials in one or more neurons that are activated by their nicotinic inputs. The possibility that these responses reflect GABA release induced by presynaptic nicotinic receptors on GABAergic terminals cannot be excluded, however. If mediated by activation of interneurons, the likely amplitude variation of nicotinic EPSPs and the relatively constant IPSC latencies

suggest an amplification of the nicotinic EPSPs by a regenerative intrinsic mechanism such as a low-threshold spike.

The identity of these hypothesized recurrent interneurons remains unknown. Recurrent IPSCs can be elicited in ChIs in the absence of triggering GABAergic inhibition in MSNs, suggesting that the interneurons that contribute to the response in MSNs *are not* responsible for recurrent inhibition (English et al., 2012). Therefore, recurrent interneurons (if they indeed exist) likely constitute a novel class of neurons which do not provide significant innervation of MSNs.

X. FUNCTIONAL CONSIDERATIONS

The dominant view in the literature depicts striatal GABAergic interneurons as participating in parallel feedforward inhibitory circuits, each providing temporally or otherwise specialized inhibitory inputs to MSNs (Gittis and Kreitzer, 2012; Kita, 1993; Tepper and Bolam, 2004; Tepper et al., 2004). This feedforward model was originally derived from several lines of evidence including data suggesting that all excitatory inputs to interneurons (cortical and/or thalamic inputs) were shared with MSNs (Kawaguchi, 1993; Kawaguchi et al., 1995), the demonstrated or presumed innervation of projection neurons (Gittis and Kreitzer, 2012; Koós and Tepper, 1999; Tepper and Bolam, 2004; Tepper et al., 2004), and the fact that none of these cells was known to receive feedback connections from MSNs (Koós and Tepper, 1999).

While the feedforward model remains a reasonable (although incomplete) approximation of the

functioning of FSIs and perhaps of THINs and PLTS interneurons, there are several reasons why it cannot be generalized to all GABAergic interneurons. First, there are at least three different interneuron types (FAIs, NPY-NGFs, and the putative recurrent interneurons) that receive potent, fast nicotinic cholinergic excitation. Since MSNs do not receive nicotinic inputs, the existence of these cholinergic inputs directly contradicts the feedforward model. Second, both ChIs and THINs receive fast synaptic inputs from MSNs. Of particular significance the innervation of THINs by MSNs is surprisingly dense and far more powerful than the weak collateral inhibition among MSNs themselves (Koós et al., 2004; Tunstall et al., 2002). Consequently, through direct and indirect circuits, MSNs exert an inhibitory feedback on THINs and the GABAergic interneurons that are innervated by ChIs. Finally, there is increasing evidence that several interneuron types are synaptically and electrotonically interconnected. These observations suggest that at least a subset of striatal GABAergic interneurons may be better conceptualized as elements in a multidirectional circuitry in which functionally distinct GABAergic interneurons, ChIs, and MSNs are interconnected through feedforward, feedback, and lateral connections.

Considering the nearly universal role of interneuronal inhibition in the oscillatory synchronization of projection neuron activity in cortical structures (Buzsáki and Wang, 2012), it is reasonable to assume that interneurons and their networks play analogous roles in the striatum. Further, although several types of interneurons exhibit intrinsic resonance at frequency ranges that are relevant for normal and pathological functioning of the basal ganglia (Beatty et al., 2015; Sciamanna and Wilson, 2011), it is likely that the emergence and regulation of oscillatory local field potentials (LFPs) and the entrainment of spike firing in various cell types also depend on complex synaptic and electrotonic interactions among interneurons and perhaps MSNs as well. For example, it has been surprisingly difficult to detect monosynaptic inhibition of MSNs by putative FSIs in vivo (Gage et al., 2010) despite the strong inhibition seen in vitro (Koós and Tepper, 1999). Similarly, while FSIs phase-lock to low- and high-frequency gamma oscillation of the LFP in the striatum (Berke, 2009), synchronized phase locking of spiking in MSNs is more difficult to demonstrate and seems to occur only during brief episodes of high-amplitude gamma oscillations in the LFP (Popescu et al., 2009). It is thus possible that the emergence of large-amplitude gamma oscillations and the transient phase locking of MSNs and FSIs reflects a change in the efficacy of inhibitory transmission from FSIs to MSNs.

One attractive candidate regulatory mechanism may be the strong muscarinic presynaptic inhibition of

transmission between FSIs and MSNs (Koós and Tepper, 2002). Since ChIs briefly stop firing in response to the presentation of a conditioned stimuli or primary reinforcement, the pause in ACh release may relieve FSIs from presynaptic inhibition resulting in increased FSI synchronization and stronger and more convergent inhibition of MSNs leading to their oscillatory entrainment. Consistent with this possibility, the pause response of ChIs and transient oscillatory entrainment of MSN firing after a conditioned stimulus (CS) (Popescu et al., 2009) emerge on a similar timescale during learning.

Further, since in vitro FSIs exhibit resonance only at a single frequency (low-gamma) (Sciamanna and Wilson, 2011), the reinforcement-dependent switching from low- to high-frequency gamma LFP oscillations observed in vivo (Berke, 2009) is probably not a cell autonomous phenomenon but represents instead a dynamic state transition within a network of interacting neurons, or is mediated by selective recruitment of distinct interneuron populations. Consistent with this argument, many putative FSIs synchronize their firing with only one of the gamma frequency bands and not with both (Berke, 2009).

Considering the high likelihood that among the neurons classified as FSIs in in vivo studies at least some are other types of GABAergic interneurons, it is possible that high-frequency gamma oscillations are driven by the recruitment of a cell type other than FSIs. In turn, the gamma frequency state transition may be controlled by rapid dopaminergic neuromodulatory effects on the intrinsic properties or synaptic connectivity of specific interneurons. Interestingly, DA induces dramatic depolarizing state transitions in THINs, a phenomenon that may have direct implications for the frequency transitions in the striatal LFP.

XI. SUMMARY AND CONCLUSIONS

It is clear that the striatum enjoys a much richer diversity of GABAergic interneurons than was once thought. We are only now beginning to discover the functional differences between the varieties of these interneurons. As new molecular, anatomical, and physiological techniques continue to become available, particularly more strains of transgenic mice that selectively label neurons that express CR and other peptides, receptors and neuroactive agents expressed by striatal neurons with fluorescent markers such as EGFP and/or express molecular tools such as Cre recombinase, it is almost certain that the number of different striatal GABAergic interneurons, currently numbering at least 10, will grow.

Acknowledgments

We thank Ms. Fulva Shah for excellent technical assistance, help with the photomicroscopy, and editorial assistance. The writing of this review and some of the research described in it were supported by NIH grants NS034865 (JMT), NS072950 (TK and JMT), and Rutgers University.

References

- Alkondon, M., Albuquerque, E.X., 1993. Diversity of nicotinic acetylcholine receptors in rat hippocampal neurons. I. Pharmacological and functional evidence for distinct structural subtypes. *J. Pharmacol. Exp. Ther.* 265, 1455–1473.
- Aoki, C., Pickel, V.M., 1988. Neuropeptide Y-containing neurons in the rat striatum: ultrastructure and cellular relations with tyrosine hydroxylase-containing terminals and with astrocytes. *Brain Res.* 459, 205–225.
- Aosaki, T., Tsubokawa, H., Ishida, A., Watanabe, K., Graybiel, A.M., Kimura, M., 1994. Responses of tonically active neurons in the primate's striatum undergo systematic changes during behavioral sensorimotor conditioning. *J. Neurosci.* 14, 3969–3984.
- Beatty, J.A., Song, S.C., Wilson, C.J., 2015. Cell-type-specific resonances shape the responses of striatal neurons to synaptic input. *J. Neurophysiol.* 113, 688–700.
- Beatty, J.A., Sullivan, M.A., Morikawa, H., Wilson, C.J., 2012. Complex autonomous firing patterns of striatal low-threshold spike interneurons. *J. Neurophysiol.* 108, 771–781.
- Bennett, B.D., Bolam, J.P., 1993. Characterization of calretinin-immunoreactive structures in the striatum of the rat. *Brain Res.* 609, 137–148.
- Bennett, B.D., Bolam, J.P., 1994. Synaptic input and output of parvalbumin-immunoreactive neurons in the neostriatum of the rat. *Neuroscience.* 62, 707–719.
- Berke, J.D., 2008. Uncoordinated firing rate changes of striatal fast-spiking interneurons during behavioral task performance. *J. Neurosci.* 28, 10075–10080.
- Berke, J.D., 2009. Fast oscillations in cortical-striatal networks switch frequency following rewarding events and stimulant drugs. *Eur. J. Neurosci.* 30, 848–859.
- Berke, J.D., 2011. Functional properties of striatal fast-spiking interneurons. *Front. Syst. Neurosci.* 5, 45.
- Berke, J.D., Okatan, M., Skurski, J., Eichenbaum, H.B., 2004. Oscillatory entrainment of striatal neurons in freely moving rats. *Neuron.* 43, 883–896.
- Betarbet, R., Turner, R., Chockkan, V., DeLong, M.R., Allers, K.A., Walters, J., Levey, A.I., Greenamyre, J.T., 1997. Dopaminergic neurons intrinsic to the primate striatum. *J. Neurosci.* 17, 67616768.
- Bevan, M.D., Booth, P.A., Eaton, S.A., Bolam, J.P., 1998. Selective innervation of neostriatal interneurons by a subclass of neuron in the globus pallidus of the rat. *J. Neurosci.* 18, 9438–9452.
- Bolam, J.P., Clarke, D.J., Smith, A.D., Somogyi, P., 1983. A type of aspiny neuron in the rat neostriatum accumulates [3H] gamma-aminobutyric acid: combination of Golgi-staining, autoradiography, and electron microscopy. *J. Comp. Neurol.* 213, 121–134.
- Bolam, J.P., Powell, J.F., Wu, J.Y., Smith, A.D., 1985. Glutamate decarboxylase-immunoreactive structures in the rat neostriatum: a correlated light and electron microscopic study including a combination of Golgi impregnation with immunocytochemistry. *J. Comp. Neurol.* 237, 1–20.
- Bracci, E., Centonze, D., Bernardi, G., Calabresi, P., 2002. Dopamine excites fast-spiking interneurons in the striatum. *J. Neurophysiol.* 87, 2190–2194.
- Bracci, E., Centonze, D., Bernardi, G., Calabresi, P., 2003. Voltage-dependent membrane potential oscillations of rat striatal fast-spiking interneurons. *J. Physiol.* 549, 121–130.
- Buzsaki, G., Wang, X.J., 2012. Mechanisms of gamma oscillations. *Annu. Rev. Neurosci.* 35, 203–225.
- Centonze, D., Bracci, E., Pisani, A., Gubellini, P., Bernardi, G., Calabresi, P., 2002. Activation of dopamine D1-like receptors excites LTS interneurons of the striatum. *Eur. J. Neurosci.* 15, 2049–2052.
- Centonze, D., Grande, C., Usiello, A., Gubellini, P., Erbs, E., Martin, A.B., Pisani, A., Tognazzi, N., Bernardi, G., Moratalla, R., Borrelli, E., Calabresi, P., 2003. Receptor subtypes involved in the presynaptic and postsynaptic actions of dopamine on striatal interneurons. *J. Neurosci.* 23, 6245–6254.
- Chang, H.T., Kita, H., 1992. Interneurons in the rat striatum: relationships between parvalbumin neurons and cholinergic neurons. *Brain Res.* 574, 307–311.
- Chesselet, M.F., Graybiel, A.M., 1986. Striatal neurons expressing somatostatin-like immunoreactivity: evidence for a peptidergic interneuronal system in the cat. *Neuroscience.* 17, 547–571.
- Chesselet, M.F., Robbins, E., 1989. Characterization of striatal neurons expressing high levels of glutamic acid decarboxylase messenger RNA. *Brain Res.* 492, 237–244.
- Cossette, M., Levesque, D., Parent, A., 2005. Neurochemical characterization of dopaminergic neurons in human striatum. *Parkinsonism Relat. Disord.* 11, 277–286.
- Cowan, R.L., Wilson, C.J., Emson, P.C., Heizmann, C.W., 1990. Parvalbumin-containing GABAergic interneurons in the rat neostriatum. *J. Comp. Neurol.* 302, 197–205.
- Czubayko, U., Plenz, D., 2002. Fast synaptic transmission between striatal spiny projection neurons. *Proc. Natl. Acad. Sci. U.S.A.* 99 (24), 15764–15769.
- Darmopil, S., Muneton-Gomez, V.C., de Ceballos, M.L., Bernson, M., Moratalla, R., 2008. Tyrosine hydroxylase cells appearing in the mouse striatum after dopamine denervation are likely to be projection neurones regulated by l-DOPA. *Eur. J. Neurosci.* 27, 580–592.
- Dautan, D., Huerta-Ocampo, I., Witten, I.B., Deisseroth, K., Bolam, J.P., Gerdjikov, T., Mena-Segovia, J., 2014. A major external source of cholinergic innervation of the striatum and nucleus accumbens originates in the brainstem. *J. Neurosci.* 34, 4509–4518.
- Dehorter, N., Guigoni, C., Hirsch, J., Eusebio, A., Ben-Ari, Y., Hammond, C., 2009. Dopamine-deprived striatal GABAergic interneurons burst and generate repetitive gigantic IPSCs in medium spiny neurons. *J. Neurosci.* 29, 7776–7787.
- Dubach, M., Schmidt, R., Kunkel, D., Bowden, D.M., Martin, R., German, D.C., 1987. Primate neostriatal neurons containing tyrosine hydroxylase: immunohistochemical evidence. *Neurosci. Lett.* 75, 205–210.
- English, D.F., Ibanez-Sandoval, O., Stark, E., Tecuapetla, F., Buzsaki, G., Deisseroth, K., Tepper, J.M., Koós, T., 2012. GABAergic circuits mediate the reinforcement-related signals of striatal cholinergic interneurons. *Nat. Neurosci.* 15, 123–130.
- Faust, T.W., Assous, M., Shah, F., Tepper, J.M., Koós, T., 2015. Novel fast adapting interneurons mediate cholinergic-induced fast GABA_A inhibitory postsynaptic currents in striatal spiny neurons. *Eur. J. Neurosci.* 42, 1764–1774.
- Figueredo-Cardenas, G., Morello, M., Sancesario, G., Bernardi, G., Reiner, A., 1996. Colocalization of somatostatin, neuropeptide Y, neuronal nitric oxide synthase and NADPH-diaphorase in striatal interneurons in rats. *Brain Res.* 735, 317–324.
- Fleig, A., Penner, R., 2004. The TRPM ion channel subfamily: molecular, biophysical and functional features. *Trends Pharmacol. Sci.* 25, 633–639.

- Freiman, I., Anton, A., Monyer, H., Urbanski, M.J., Szabo, B., 2006. Analysis of the effects of cannabinoids on identified synaptic connections in the caudate-putamen by paired recordings in transgenic mice. *J. Physiol.* 575, 789–806.
- Freund, T.F., Buzsaki, G., 1996. Interneurons of the hippocampus. *Hippocampus*. 6, 347–470.
- Fuentealba, P., Begum, R., Capogna, M., Jinno, S., Marton, L.F., Csicsvari, J., Thomson, A., Somogyi, P., Klausberger, T., 2008. Ivy cells: a population of nitric-oxide-producing, slow-spiking GABAergic neurons and their involvement in hippocampal network activity. *Neuron*. 57, 917–929.
- Gage, G.J., Stoetzer, C.R., Wiltschko, A.B., Berke, J.D., 2010. Selective activation of striatal fast-spiking interneurons during choice execution. *Neuron*. 67, 466–479.
- Galarreta, M., Hestrin, S., 1999. A network of fast-spiking cells in the neocortex connected by electrical synapses. *Nature*. 402, 72–75.
- Galarreta, M., Hestrin, S., 2001. Electrical synapses between GABA-releasing interneurons. *Nat. Rev. Neurosci.* 2, 425–433.
- Galarreta, M., Hestrin, S., 2002. Electrical and chemical synapses among parvalbumin fast-spiking GABAergic interneurons in adult mouse neocortex. *Proc. Natl. Acad. Sci. U.S.A.* 99, 12438–12443.
- Gerfen, C.R., Paletzki, R., Heintz, N., 2013. GENSAT BAG Cre-Recombinase driver lines to study the functional organization of cerebral cortical and basal ganglia circuits. *Neuron*. 80, 1368–1383.
- Gittis, A.H., Kreitzer, A.C., 2012. Striatal microcircuitry and movement disorders. *Trends Neurosci.* 35, 557–564.
- Gittis, A.H., Leventhal, D.K., Fensterheim, B.A., Pettibone, J.R., Berke, J.D., Kreitzer, A.C., 2011. Selective inhibition of striatal fast-spiking interneurons causes dyskinesias. *J. Neurosci.* 31, 15727–15731.
- Gittis, A.H., Nelson, A.B., Thwin, M.T., Palop, J.J., Kreitzer, A.C., 2010. Distinct roles of GABAergic interneurons in the regulation of striatal output pathways. *J. Neurosci.* 30, 2223–2234.
- Gong, S., Zheng, C., Doughty, M.L., Losos, K., Didkovsky, N., Schambra, U.B., Nowak, N.J., Joyner, A., Leblanc, G., Hatten, M.E., Heintz, N., 2003. A gene expression atlas of the central nervous system based on bacterial artificial chromosomes. *Nature*. 425, 917–925.
- Gustafson, N., Gireesh-Dharmaraj, E., Czabayko, U., Blackwell, K.T., Plenz, D., 2006. A comparative voltage and current-clamp analysis of feedback and feedforward synaptic transmission in the striatal microcircuit in vitro. *J. Neurophysiol.* 95, 737–752.
- Guzman, J.N., Hernandez, A., Galarraga, E., Tapia, D., Laville, A., Vergara, R., Aceves, J., Vargas, J., 2003. Dopaminergic modulation of axon collaterals interconnecting spiny neurons of the rat striatum. *J. Neurosci.* 23, 8931–8940.
- Hill, K., Benham, C.D., McNulty, S., Randall, A.D., 2004. Flufenamic acid is a pH-dependent antagonist of TRPM2 channels. *Neuropharmacology*. 47, 450–460.
- Huot, P., Lévesque, M., Parent, A., 2007. The fate of striatal dopaminergic neurons in Parkinson's disease and Huntington's chorea. *Brain*. 130, 222–232.
- Huot, P., Parent, A., 2007. Dopaminergic neurons intrinsic to the striatum. *J. Neurochem.* 101, 1441–1447.
- Ibanez-Sandoval, O., Tecuapetla, F., Unal, B., Shah, F., Koós, T., Tepper, J.M., 2010. Electrophysiological and morphological characteristics and synaptic connectivity of tyrosine hydroxylase-expressing neurons in adult mouse striatum. *J. Neurosci.* 30, 6999–7016.
- Ibanez-Sandoval, O., Tecuapetla, F., Unal, B., Shah, F., Koós, T., Tepper, J.M., 2011. A novel functionally distinct subtype of striatal neuropeptide Y interneuron. *J. Neurosci.* 31, 16757–16769.
- Ibanez-Sandoval, O., Xenias, H.S., Tepper, J.M., Koós, T., 2015. Dopaminergic and cholinergic modulation of striatal tyrosine hydroxylase interneurons. *Neuropharmacology*. 95, 468–476.
- Kalanithi, P.S., Zheng, W., Kataoka, Y., DiFiglia, M., Grantz, H., Saper, C.B., Schwartz, M.L., Leckman, J.F., Vaccarino, F.M., 2005. Altered parvalbumin-positive neuron distribution in basal ganglia of individuals with Tourette syndrome. *Proc. Natl. Acad. Sci. U.S.A.* 102, 13307–13312.
- Kawaguchi, Y., 1993. Physiological, morphological, and histochemical characterization of three classes of interneurons in rat neostriatum. *J. Neurosci.* 13, 4908–4923.
- Kawaguchi, Y., Wilson, C.J., Augood, S.J., Emson, P.C., 1995. Striatal interneurons: chemical, physiological and morphological characterization. *Trends Neurosci.* 18, 527–535.
- Khibnik, L.A., Tritsch, N.X., Sabatini, B.L., 2014. A direct projection from mouse primary visual cortex to dorsomedial striatum. *PLoS One*. 9, e104501.
- Kincaid, A.E., Zheng, T., Wilson, C.J., 1998. Connectivity and convergence of single corticostriatal axons. *J. Neurosci.* 18, 4722–4731.
- Kita, H., 1993. GABAergic circuits of the striatum. *Prog. Brain Res.* 99, 51–72.
- Kita, H., Kita, T., 2011. Role of striatum in the pause and burst generation in the globus pallidus of 6-OHDA-treated rats. *Front. Syst. Neurosci.* 5, 42.
- Kita, H., Kosaka, T., Heizmann, C.W., 1990. Parvalbumin-immunoreactive neurons in the rat neostriatum: a light and electron microscopic study. *Brain Res.* 536, 1–15.
- Klaus, A., Planert, H., Hjorth, J., Berke, J.D., Silberberg, G., Kotaleski, J.H., 2011. Striatal fast-spiking interneurons: from firing patterns to postsynaptic impact. *Front. Syst. Neurosci.* 5, 57.
- Koós, T., Tepper, J.M., 1999. Inhibitory control of neostriatal projection neurons by GABAergic interneurons. *Nat. Neurosci.* 2, 467–472.
- Koós, T., Tepper, J.M., 2002. Dual cholinergic control of fast-spiking interneurons in the neostriatum. *J. Neurosci.* 22, 529–535.
- Koós, T., Tepper, J.M., Wilson, C.J., 2004. Comparison of IPSCs evoked by spiny and fast-spiking neurons in the neostriatum. *J. Neurosci.* 24, 7916–7922.
- Kubota, Y., Inagaki, S., Kito, S., Shimada, S., Okayama, T., Hatanaka, H., Pelletier, G., Takagi, H., Tohyama, M., 1988. Neuropeptide Y-immunoreactive neurons receive synaptic inputs from dopaminergic axon terminals in the rat neostriatum. *Brain Res.* 458, 389–393.
- Kubota, Y., Inagaki, S., Kito, S., Wu, J.Y., 1987. Dopaminergic axons directly make synapses with GABAergic neurons in the rat neostriatum. *Brain Res.* 406, 147–156.
- Kubota, Y., Kawaguchi, Y., 2000. Dependence of GABAergic synaptic areas on the interneuron type and target size. *J. Neurosci.* 20, 375–386.
- Kubota, Y., Mikawa, S., Kawaguchi, Y., 1993. Neostriatal GABAergic interneurons contain NOS, calretinin or parvalbumin. *NeuroReport*. 5, 205–208.
- Le Moine, C., Normand, E., Bloch, B., 1991. Phenotypical characterization of the rat striatal neurons expressing the D1 dopamine receptor gene. *Proc. Natl. Acad. Sci. U.S.A.* 88, 4205–4209.
- Lee, C.R., Machold, R.P., Witkovsky, P., Rice, M.E., 2013. TRPM2 channels are required for NMDA-induced burst firing and contribute to H₂O₂-dependent modulation in substantia nigra pars reticulata GABAergic neurons. *J. Neurosci.* 33, 1157–1168.
- Lee, C.R., Tepper, J.M., 2007. A calcium-activated nonselective cation conductance underlies the plateau potential in rat substantia nigra GABAergic neurons. *J. Neurosci.* 27, 6531–6541.
- Lee, S., Hjerling-Leffler, J., Zaghera, E., Fishell, G., Rudy, B., 2010. The largest group of superficial neocortical GABAergic interneurons

- expresses ionotropic serotonin receptors. *J. Neurosci.* 30, 16796–16808.
- Lenz, S., Perney, T.M., Qin, Y., Robbins, E., Chesselet, M.F., 1994. GABA-ergic interneurons of the striatum express the Shaw-like potassium channel Kv3.1. *Synapse.* 18, 55–66.
- Li, J.L., Kaneko, T., Mizuno, N., 2002. Synaptic association of dopaminergic axon terminals and neurokinin-1 receptor-expressing neurons in the striatum of the rat. *Neurosci. Lett.* 324, 9–12.
- Luk, K.C., Sadikot, A.F., 2001. GABA promotes survival but not proliferation of parvalbuminimmunoreactive interneurons in rodent neostriatum: an in vivo study with stereology. *Neuroscience.* 104, 93–103.
- Luo, R., Janssen, M.J., Partridge, J.G., Vicini, S., 2013. Direct and GABA-mediated indirect effects of nicotinic ACh receptor agonists on striatal neurones. *J. Physiol.* 591, 203–217.
- Mallet, N., Ballion, B., Le Moine, C., Gonon, F., 2006. Cortical inputs and GABA interneurons imbalance projection neurons in the striatum of parkinsonian rats. *J. Neurosci.* 26, 3875–3884.
- Mallet, N., Le Moine, C., Charpier, S., Gonon, F., 2005. Feedforward inhibition of projection neurons by fast-spiking GABA interneurons in the rat striatum in vivo. *J. Neurosci.* 25, 3857–3869.
- Mallet, N., Micklem, B.R., Henny, P., Brown, M.T., Williams, C., Bolam, J.P., Nakamura, K.C., Magill, P.J., 2012. Dichotomous organization of the external globus pallidus. *Neuron.* 74, 1075–1086.
- Mao, L., Lau, Y.S., Petroske, E., Wang, J.Q., 2001. Profound astrogenesis in the striatum of adult mice following nigrostriatal dopaminergic lesion by repeated MPTP administration. *Dev. Brain Res.* 131, 57–65.
- Marder, E., Goaillard, J.M., 2006. Variability, compensation and homeostasis in neuron and network function. *Nat. Rev. Neurosci.* 7, 563–574.
- Mazloom, M., Smith, Y., 2006. Synaptic microcircuitry of tyrosine hydroxylase-containing neurons and terminals in the striatum of 1-methyl-4-phenyl-1,2,3,6-tetrahydropyridine-treated monkeys. *J. Comp. Neurol.* 495, 453–469.
- Meredith, G.E., Farrell, T., Kellaghan, P., Tan, Y., Zahm, D.S., Totterdell, S., 1999. Immunocytochemical characterization of catecholaminergic neurons in the rat striatum following dopamine-depleting lesions. *Eur. J. Neurosci.* 11, 3585–3596.
- Misgeld, U., Drew, G., Yanovsky, Y., 2007. Presynaptic modulation of GABA release in the basal ganglia. *Prog. Brain Res.* 160, 245–259.
- Muñoz-Manchado, A.B., Foldi, C., Szydlowski, S., Sjuldo, L., Farries, M., Wilson, C., Silberberg, G., Hjerling-Leffler, J., 2014. Novel striatal GABAergic interneuron populations labeled in the 5HT3a^{EGFP} mouse. *Cereb. Cortex.* Aug 21. pii:bhu179. [Epub ahead of print].
- Narushima, M., Uchigashima, M., Hashimoto, K., Watanabe, M., Kano, M., 2006. Depolarization induced suppression of inhibition mediated by endocannabinoids at synapses from fast-spiking interneurons to medium spiny neurons in the striatum. *Eur. J. Neurosci.* 24, 2246–2252.
- Oorschot, D.E., 1996. Total number of neurons in the neostriatal, pallidal, subthalamic, and substantia nigral nuclei of the rat basal ganglia: a stereological study using the cavalieri and optical disector methods. *J. Comp. Neurol.* 366, 580–599.
- Parthasarathy, H.B., Graybiel, A.M., 1997. Cortically driven immediate-early gene expression reflects modular influence of sensorimotor cortex on identified striatal neurons in the squirrel monkey. *J. Neurosci.* 17, 2477–2491.
- Partridge, J.G., Janssen, M.J., Chou, D.Y., Abe, K., Zukowska, Z., Vicini, S., 2009. Excitatory and inhibitory synapses in neuropeptide Y-expressing striatal interneurons. *J. Neurophysiol.* 102, 3038–3045.
- Perk, C.G., Wickens, J.R., Hyland, B.I., 2015. Differing properties of putative fast-spiking interneurons in the striatum of two rat strains. *Neuroscience.* 294, 215–226.
- Petilla Interneuron Nomenclature Group, 2008. Petilla terminology: nomenclature of features of GABAergic interneurons of the cerebral cortex. *Nat. Rev. Neurosci.* 9, 557–568.
- Petroske, E., Meredith, G.E., Callen, S., Totterdell, S., Lau, Y.S., 2001. Mouse model of Parkinsonism: a comparison between subacute MPTP and chronic MPTP/probenecid treatment. *Neuroscience.* 106, 589–601.
- Planert, H., Szydlowski, S.N., Hjorth, J.J., Grillner, S., Silberberg, G., 2010. Dynamics of synaptic transmission between fast-spiking interneurons and striatal projection neurons of the direct and indirect pathways. *J. Neurosci.* 30, 3499–3507.
- Plenz, D., Kitai, S.T., 1998. Up and down states in striatal medium spiny neurons simultaneously recorded with spontaneous activity in fast-spiking interneurons studied in cortex-striatum substantia nigra organotypic cultures. *J. Neurosci.* 18, 266–283.
- Plotkin, J.L., Wu, N., Chesselet, M.F., Levine, M.S., 2005. Functional and molecular development of striatal fast-spiking GABAergic interneurons and their cortical inputs. *Eur. J. Neurosci.* 22, 1097–1108.
- Popescu, A.T., Popa, D., Pare, D., 2009. Coherent gamma oscillations couple the amygdala and striatum during learning. *Nat. Neurosci.* 12, 801–807.
- Porritt, M.J., Batchelor, P.E., Hughes, A.J., Kalnins, R., Donnan, G.A., Howells, D.W., 2000. New dopaminergic neurons in Parkinson's disease striatum. *Lancet.* 356, 44–45.
- Prensa, L., Gimenez-Amaya, J.M., Parent, A., 1998. Morphological features of neurons containing calcium-binding proteins in the human striatum. *J. Comp. Neurol.* 390, 552–563.
- Price, C.J., Cauli, B., Kovacs, E.R., Kulik, A., Lambolez, B., Shigemoto, R., Capogna, M., 2005. Neurogliaform neurons form a novel inhibitory network in the hippocampal CA1 area. *J. Neurosci.* 25, 6775–6786.
- Ramanathan, S., Hanley, J.J., Deniau, J.M., Bolam, J.P., 2002. Synaptic convergence of motor and somatosensory cortical afferents onto GABAergic interneurons in the rat striatum. *J. Neurosci.* 22, 8158–8169.
- Reig, R., Silberberg, G., 2014. Multisensory integration in the mouse striatum. *Neuron.* 83, 1200–1212.
- Rivera, A., Alberti, I., Martin, A.B., Narvaez, J.A., de la Calle, A., Moratalla, R., 2002. Molecular phenotype of rat striatal neurons expressing the dopamine D5 receptor subtype. *Eur. J. Neurosci.* 16, 2049–2058.
- Rudy, B., Fishell, G., Lee, S., Hjerling-Leffler, J., 2011. Three groups of interneurons account for nearly 100% of neocortical GABAergic neurons. *Dev. Neurobiol.* 71, 45–61.
- Rudy, B., McBain, C.J., 2001. Kv3 channels: voltage-gated K⁺ channels designed for high-frequency repetitive firing. *Trends Neurosci.* 24, 517–526.
- Rymar, V.V., Sasseville, R., Luk, K.C., Sadikot, A.F., 2004. Neurogenesis and stereological morphometry of calretinin-immunoreactive GABAergic interneurons of the neostriatum. *J. Comp. Neurol.* 469, 325–339.
- Schultz, W., Ungerstedt, U., 1978. Short-term increase and long-term reversion of striatal cell activity after degeneration of the nigrostriatal dopamine system. *Exp. Brain Res.* 33, 159–171.
- Sciamanna, G., Wilson, C.J., 2011. The ionic mechanism of gamma resonance in rat striatal fast-spiking neurons. *J. Neurophysiol.* 106, 2936–2949.
- Shah, F., Faust, T., Unal, B., Koós, T., Tepper, J.M., 2012. Anatomical and electrophysiological studies of striatal calretinin-expressing interneurons in mice. *Soc. Neurosci. Abstr.* 38 (790), 21.

- Sharott, A., Doig, N.M., Mallet, N., Magill, P.J., 2012. Relationships between the firing of identified striatal interneurons and spontaneous and driven cortical activities in vivo. *J. Neurosci.* 32, 13221–13236.
- Sullivan, M.A., Chen, H., Morikawa, H., 2008. Recurrent inhibitory network among striatal cholinergic interneurons. *J. Neurosci.* 28, 8682–8690.
- Szydlowski, S.N., Pollak Dorocic, I., Planert, H., Carlen, M., Meletis, K., Silberberg, G., 2013. Target selectivity of feedforward inhibition by striatal fast-spiking interneurons. *J. Neurosci.* 33, 1678–1683.
- Tande, D., Hoglinger, G., Debeir, T., Freundlieb, N., Hirsch, E.C., Francois, C., 2006. New striatal dopamine neurons in MPTP-treated macaques result from a phenotypic shift and not neurogenesis. *Brain.* 129, 1194–1200.
- Tashiro, Y., Kaneko, T., Sugimoto, T., Nagatsu, I., Kikuchi, H., Mizuno, N., 1989a. Striatal neurons with aromatic L-amino acid decarboxylase-like immunoreactivity in the rat. *Neurosci. Lett.* 100, 29–34.
- Tashiro, Y., Sugimoto, T., Hattori, T., Uemura, Y., Nagatsu, I., Kikuchi, H., Mizuno, N., 1989b. Tyrosine hydroxylase-like immunoreactive neurons in the striatum of the rat. *Neurosci. Lett.* 97, 6–10.
- Taverna, S., Canciani, B., Pennartz, C.M., 2007. Membrane properties and synaptic connectivity of fast-spiking interneurons in rat ventral striatum. *Brain Res.* 1152, 49–56.
- Tecuapetla, F., Carrillo-Reid, L., Bargas, J., Galarraga, E., 2007. Dopaminergic modulation of short-term synaptic plasticity at striatal inhibitory synapses. *Proc. Natl. Acad. Sci. U.S.A.* 104, 10258–10263.
- Tecuapetla, F., Carrillo-Reid, L., Guzman, J.N., Galarraga, E., Bargas, J., 2005. Different inhibitory inputs onto neostriatal projection neurons as revealed by field stimulation. *J. Neurophysiol.* 93, 1119–1126.
- Tecuapetla, F., Koós, T., Tepper, J.M., Kabbani, N., Yeckel, M.F., 2009. Differential dopaminergic modulation of neostriatal synaptic connections of striatopallidal axon collaterals. *J. Neurosci.* 29, 8977–8990.
- Tepper, J.M., Bolam, J.P., 2004. Functional diversity and specificity of neostriatal interneurons. *Curr. Opin. Neurobiol.* 14, 685–692.
- Tepper, J.M., Koós, T., Wilson, C.J., 2004. GABAergic microcircuits in the neostriatum. *Trends Neurosci.* 27, 662–669.
- Tepper, J.M., Tecuapetla, F., Koós, T., Ibanez-Sandoval, O., 2010. Heterogeneity and diversity of striatal GABAergic interneurons. *Front. Neuroanat.* 4, 150.
- Tepper, J.M., Wilson, C.J., Koós, T., 2008. Feedforward and feedback inhibition in neostriatal GABAergic spiny neurons. *Brain Res. Rev.* 58, 272–281.
- Tunstall, M.J., Oorschot, D.E., Kean, A., Wickens, J.R., 2002. Inhibitory interactions between spiny projection neurons in the rat striatum. *J. Neurophysiol.* 88, 1263–1269.
- Ugrumov, M.V., 2009. Non-dopaminergic neurons partly expressing dopaminergic phenotype: distribution in the brain, development and functional significance. *J. Chem. Neuroanat.* 38, 241–256.
- Unal, B., Ibanez-Sandoval, O., Shah, F., Abercrombie, E.D., Tepper, J.M., 2011. Distribution of tyrosine hydroxylase-expressing interneurons with respect to anatomical organization of the neostriatum. *Front. Syst. Neurosci.* 5, 41.
- Unal, B., Shah, F., Kothari, J., Tepper, J.M., 2015. Anatomical and electrophysiological changes in striatal TH interneurons after loss of the nigrostriatal dopaminergic pathway. *Brain Struct. Funct.* 220, 331–349.
- Vincent, S.R., Johansson, O., 1983. Striatal neurons containing both somatostatin- and avian pancreatic polypeptide (APP)-like immunoreactivities and NADPH-diaphorase activity: a light and electron microscopic study. *J. Comp. Neurol.* 217, 264–270.
- Vincent, S.R., Staines, W.A., Fibiger, H.C., 1983. Histochemical demonstration of separate populations of somatostatin and cholinergic neurons in the rat striatum. *Neurosci. Lett.* 35, 111–114.
- Wu, Y., Parent, A., 2000. Striatal interneurons expressing calretinin, parvalbumin or NADPHdiaphorase: a comparative study in the rat, monkey and human. *Brain Res.* 863, 182–191.
- Xenias, H., Ibañez-Sandoval, O., Koós, T., Tepper, J.M., 2015. Are striatal tyrosine hydroxylase interneurons dopaminergic? *J. Neurosci.* 35, 6584–6599.
- Yang, Z., You, Y., Levison, S.W., 2008. Neonatal hypoxic/ischemic brain injury induces production of calretinin-expressing interneurons in the striatum. *J. Comp. Neurol.* 511, 19–33.